CORROSION OF STEEL WELDMENT

A DISSERTATION

Submitted in partial fulfillment of the

Requirements for the award of the degree

Of

Master of Technology

In

METALLURGICAL AND MATERIALS ENGINEERING

(With specialization in Industrial Metallurgy)

By

NEERAJ KUMAR PRASAD

DEPARTMENT OF METALLURGICAL AND MATERIALS ENGINEERING

INDIAN INSTITUTE OF TECHNOLOGY ROORKEE

ROORKEE – 247 667 (INDIA)

MAY, 2016

CANDIDATE DECLARATION

I hearby declare that the work which is being presented in this dissertation entiled

"CORROSION OF STEEL WELDMENT"

In the partial fulfilment of the requirments for the award of the degree of "Master of Technology" in Matellurgical and materials Engineering with specialization in Industrial Metallurgy under the supervision of Dr. Mukesh Bhardwaj, Assistant Professor, Department of Metallurgical and Materisls Engineering, IIT Roorkee.

Date **(NEERAJ KUMAR PRASAD)**

Place: IIT Roorkee

CERTIFICATE

This is to certify that the above declaration made by the candidate is correct to the best of my knowledge.

Date **(Dr. MUKESH BHARDWAJ)**

Assistant Professor

Department of Metallurgical and Materisls Engineering

IIT Roorkee-247667

India

ACKNOWLEDGEMENT

I would like to thank god and parents for their blessings. First and foremost, I am thankful to my supervisor, Dr. Mukesh Bhardwaj, Assistant Professor, Department of Metallurgical and Materials Engineering at IIT Roorkee for being helpful and for his useful suggestions, discussions and consistant encourgement throughout the duration of this work. His trust on my ability helped me push my own limits, to produce better quality of work.

I would also like to thank our Head of the Department, Prof. Anjan Sil for providing all the facilities required to carry out the work. I would like to thank all laboratry supritendents of the Department who were actively involved in providing me constant support and motivation.

I am thankful to my friends for giving me moral and emotional support. Their patient understanding and persistent prayers have been a great source of encouregment and strengt during the process.

NEERAJ KUMAR PRASAD

IIT Roorkee

ABSTRACT

Austenitic stainless steels find important and variety application such as construction materials in chemical and petrochemical industries, civil engineering, marine, ship building, oil and gas industry. SS 316 (stainless steel 316) is one of most popular austenitic stainless steel used for these applications. Welding of stainless steels modify the constancy of the passive layer causes the corrosion issue arises when it is exposed to the industrial environment. This work is aim to determine the corrosion behavior of welded SS 316 steel under different welding parameters. Electrochemical tests (Open Circuit Potential, Linear Polarization, Cyclic Polarization and electrochemical impedance spectroscopy) are used in order to obtain the corrosion behavior of SS 316 steel. Nine welding parameters are used in this project and from every welding parameter two samples are used for investigation; welded cut section at fusion zone and cut section at HAZ (heat affected zone) of SS 316 with one base metal sample. Temperature and pH of the 3.5% NaCl solution are the parameters that involve in determining the corrosivity of the welded SS 316.

TABLE OF CONTENT

LIST OF FIGURES

LIST OF TABLES

SS 316 (Stainless steel 316) is most frequently used form of stainless steel. This steel has molybdenum and nickel percentage more than stainless steel 304. The composition of this steel gives good corrosion resistance in corrosive environment. The addition of molybdenum ascertains more to pitting and crevice corrosion resistance in chloride atmosphere, chemical environments and sea water. SS 316 offers good mechanical and corrosive resistant properties and good welding characteristics. SS 316 steel is normally used in many industrial applications related to processing chemicals, food preparation equipment particularly in chloride environments, Coastal architectural paneling, railings & trim, Chemical containers used for transport, heat exchangers, pharmaceutical industry and high-saline environments such as coastal regions and outdoor areas. Due to its nonreactive qualities, SS 316 steel is also used in the manufacturing of medical surgical instruments.

1. 1 CORROSION RESISTANCE

SS 316 is more corrosion resistant than SS 304. SS 316 has good corrosion resistance to most complex sulfur compound found in paper and pulp industries.
SS 316 has good pitting corrosion resistance also in acetic acid and phosphoric acid. SS 316 has exceptional corrosion resistance to marine environment.

1.2 ATMOSPHERIC CORROSION

SS 316 has good atmospheric corrosion resistance over other uncoated materials. Addition of molybdenum gives resistance to pitting and staining. For this reason this grade material is used in aggressive chloride environment.

1.3 STRESS CORROSION CRACKING (SCC)

Stress corrosion cracking can arise in SS 316 steel, when steel is stressed in tension in chloride atmosphere. The stress present in the system may be applied stress or residual stresses generated during welding and cold working.

1.4 INTERGRANULAR CORROSION

Sensitization problem may arise in heat affected zone of weldment when weld of stainless steel 316 is cooled through sensitization temperature, at this temperature composition may change at grain boundaries. If a SS 316 with sensitization problem is exposed to corrosive environment, it may be possible an intergranular attack.

1.5 WELDING

Welding is generally used to fabricate stainless steel structures. The welding method has been used in different applications for example, automotive exhaust gas systems, pipelines, chemical industrial equipment [1][2] But, welding often has effects on the microstructure and therefore is likely to have tough influence on the corrosion and mechanical properties of the welded samples. Welding process produces different metallurgical problems such as presence of porosities, precipitation of secondary phases, micro segregation, loss of materials by vaporization and cracking [3]. It is well-known that the microstructure of austenitic stainless steel is primarily composed of austenite under the situation of equilibrium solidification. on the other hand, during the non equilibrium quick solidification conditions, such as in welding, incomplete transformation will takes place at high cooling rate and small amounts of δ ferrite should be remained inevitably in the weld microstructure at room temperature. The retained δ ferrite is known to prevent hot cracking and solidification to improve toughness, ductility, and corrosion resistance. However, it is also reported that excess δ ferrite (usually more than 10 vol. %) can decrease the hot workability [4]. Therefore, δ ferrite content in the weldment plays an important role in the welding of austenitic stainless steels which should be controlled.

It is likely that the welding processes can alter the passivity due to thermal cycles and compositional changes due to welding. Stainless steel weldment corrosion has been the topic of significant research. Inter granular corrosion due to sensitization is one of the most common problem in stainless steel weldment. This is a well known fact due to inter-metallic phases and precipitation of carbides at grain boundaries, through heating in the range, usually 600– 850 ^{0}C (sensitization temperature range). It may be possible a change in composition of the welded

material by fusion welding, which can modify the stability of the passive layer and corrosion behavior [5].

2.1 WELDMENT

Weldment reveals unusual micro structural features that need to be acknowledged and understood in order to forecast satisfactory corrosion service life of welded structures [6].

Weldment inherently own compositional and micro structural difference, which can be categorized by dimensional scale. On the major scale, a weldment consists of a transition from base metal, heat affected zone and solidified weld metal zone of fusion zone and includes five micro structurally distinct regions normally identified [6] as fusion zone, unmixed region, partially melted region, heat affected zone, and the base metal.

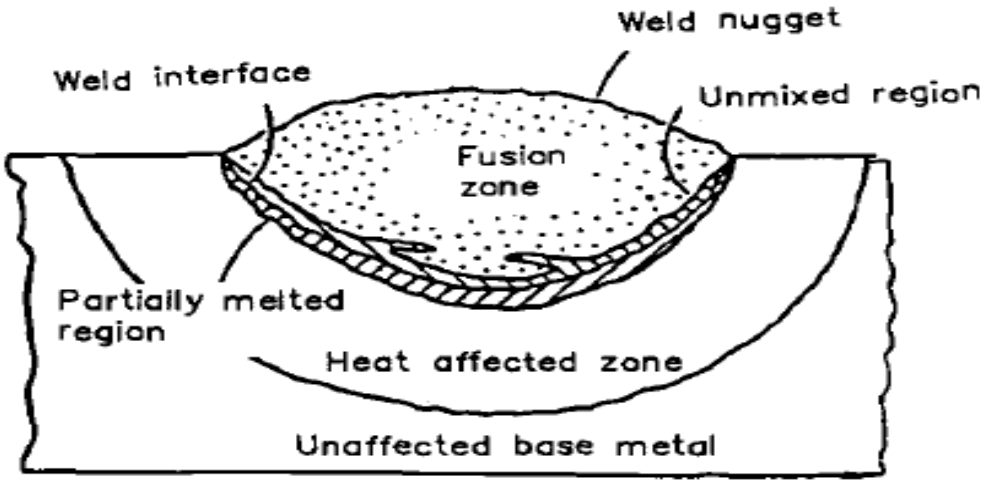

Fig.1 Schematic of weldment showing all different zones[6]

2.2 CORROSIONS IN WELDMENTS

Weldment can practice all types of corrosion, but they are mainly inclined to those influenced by dissimilarity in microstructure and composition. Particularly, pitting, galvanic corrosion, stress corrosion, hydrogen cracking and intergranular corrosion.

2.3 WELD DECAY OF STAINLESS STEEL

At some stage in welding of stainless steels, local sensitized zones frequently develop. Sensitization is because of the growth of chromium carbide alongside grain boundaries, ensuing in reduction of chromium in the area neighboring to the grain boundary[6]. This reduction in chromium produces much localized galvanic cells. but this reduction jump downs the chromium under the compulsory 12 wt% that is needed to sustain a protective passive film, the area will turn into sensitized to corrosion, following intergranular attack. This kind of corrosion mainly frequently occurs in the heat-affected zone. Intergranular corrosion is a reason to loss of metal parallel to weld deposit in that area. This corrosion activity is known as weld decay [7].

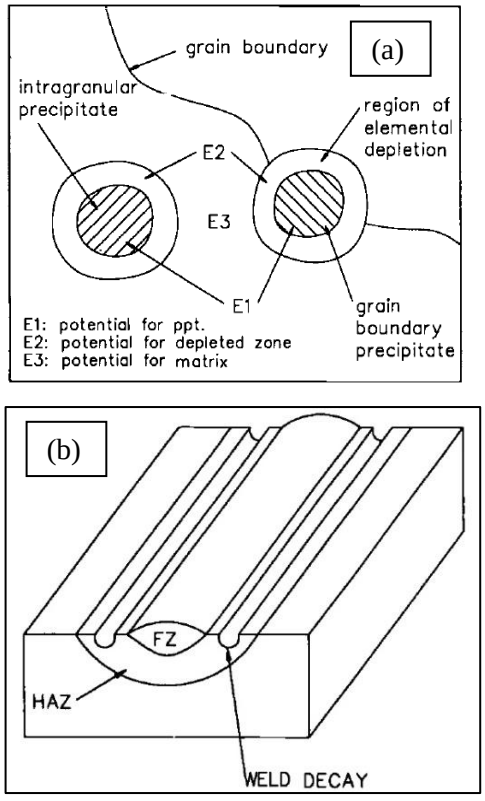

Fig. 2 (a) Depleted regions adjacent to precipitates. (b) Inter-granular of stainless steel

2.4 ROLE OF DELTA (δ) FERRITE IN STAINLESS STEEL WELDMENT

The microstructure of austenitic stainless steel is mainly has austenite when solidifies at equilibrium condition. On the other hand, during the non-equilibrium quick solidification conditions, such as in welding, incomplete transformation takes place due to high cooling rate and small amounts of δ ferrite remains inevitably in the weld microstructure at room temperature. The retained δ ferrite is known to prevent hot cracking during solidification and to enhance ductility, toughness and corrosion resistance. On the other hand, it is also stated that surplus δ ferrite, generally more than 10 vol. %. Hot workability may be decreased [4]. So δ ferrite content in the weldment plays an important role in the welding of austenitic stainless steels which should be controlled.

2.5 EFFECT OF PRE HEATING ON STEEL WELDMENT

It has been reported that near the heat source of welding, preheating generally disturbs the temperature distribution, and revises cooling rate and temperature gradient of weldment. In comparison with other dimensions plates have a small thickness because of this a two-dimensional Rosenthal equation was used around the welding torch to calculate the quasi stationary temperature distribution [8]. Using MATLAB software by Rosenthal equation, isothermal contours were obtained around the heat source [9]. Where isothermal contours elongate due to increase in preheating temperature. It was reported that if welding speed is fixed, there is a reduction of a specific temperature interval, which confirms by elongation of contours and because of this welding torch required to move over more area of weldment. In another word, it has been conclude that a reduction of average temperature gradient with increment of preheating temperature will go along. a product of welding speed and temperature gradient is defined as the cooling rate of welds, the constant welding speed directly proportional to average temperature gradient and average cooling rate, it means if we will raise the preheating temperature there will be decrease in cooling rate. The calculated cooling curves of heat affected zone and weld pool which were acquired by thermocouples verify the earlier estimation. It can be observe from the figure that, the sample which were preheated at temperature 650 ^{0}C has slightest cooling rate, weldment without preheating cools quickly. For solid state transformation of ferrite to austenite high temperature cooling rate of weld pool is a dominant parameter, in this temperature interval, cooling curves are reported. It is mentioned that through preheating slow down the cooling rate of heat affected zone, there is a possibility of increases in carbides formation in area which is not suitable for weldment. On the other hand, even through preheating temperature at 650 ^{0}C, where heat affected zone slowly cools, the cooling time is still far shorter than 500 min stated by Davidson et al.[9].from sensitization temperature interval, 600 ^{0}C to 900 ^{0}C, It can be conclude that heat affected zone does not sensitize by preheating of welds. To characterize the phases in heat affected zone, sample was tested at long time per step over a small scan area in X Ray Diffraction. Obtained result at heat affected zone proves no carbide formation, and hold up the assessment made by thermal analysis.

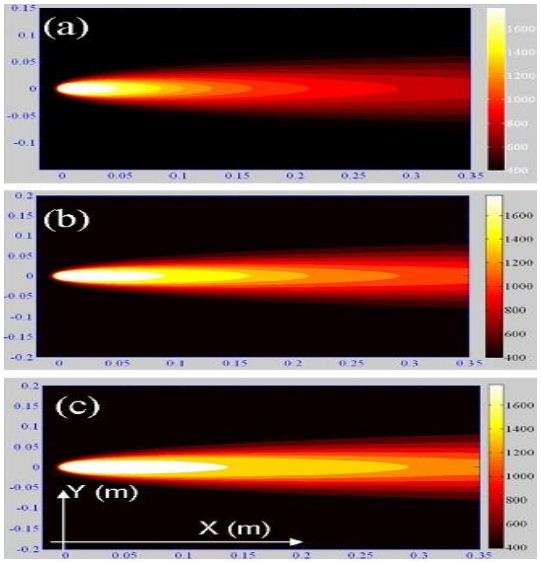

Fig.3 Preheating temperature effect, near welding torch (a) no preheating, (b) preheated by 450 ^{0}C (c) preheated by 650 ^{0}C. [17]

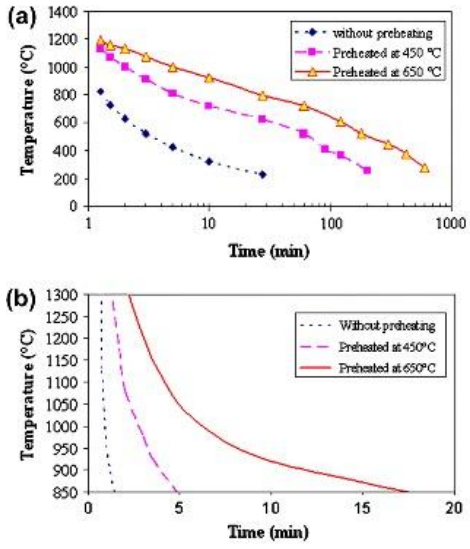

Fig. 4 (a) Cooling curve for fusion zone. (b) Cooling curve for heat affected zone

2.6 EFFECT OF WELDING SPEED ON STEEL WELDMENT [10]

It was reported that the width of face and root of weld reduced with increase in welding speed. Because of weld pool have low heat input in the **Fig.** 5. Considerable grain growth is found in HAZ of all the weldment and it is also observes that with increase in welding speed, the size of grain coarsening decreases.

It was found, smaller size dendrite in the fusion zone at 3.5 mm/s welding speed weldment than at 2.5 mm/s welding speed and at 1.5 mm/s welding speed weldments, and it was found that maximum ductility and tensile strength are possessed by weldment which is welded at welding speed3.5 mm/s.

Pitting corrosion potential increased with welding speed of weld metal due to less inter-dendrite spacing and small dendrite sizes in the fusion zone.

It was also found that harden of the base metal is higher than that of weld metal by all the weldments and it was also experienced that with increase in welding speed, hardness values of weld metals increases.

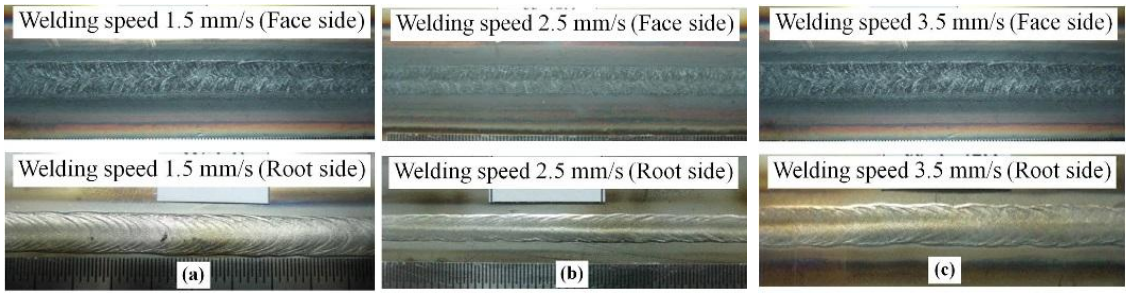

Fig.5 Weldment face and root side, obtained using different welding speed: (a)1.5 mm/s (b) 2.5 mm (c) 3.5 mm/s. [10]

2.7 EFFECT OF HEAT INPUT WITH WELDING SPEED ON STEEL WELDMENT

It was articulated by M. Pujar et. al. that at lower heat input very fine ferrite was present and as the heat input increased it get coarsened. Also found that at lower heat input corrosion rate is dependent of pitting potential and at higher heat input it is independent of pitting potential. 20 V welding voltage, 200 A welding current, 6L/min argon flow rate, these were the welding parameters used for welding 25 mm thick plate of SS 316 by GTAW (Gas Tungsten Arc Welding) [11]

P. Giridharan et. al. stated the behavior of SS 304 L welded through pulsed GTAW. Welding speed were 1.83, 2.10, 2.50, 2.90 and 3.10 mm/s with pulse current of 180, 188, 200, 212 and 220 A and 450, 490, 550,610 and 650 were the pulse current duration. Welding voltage was 14 V. It was found that cooling rate of top surface decreases with the increase in pulse current, hence stability of passive layer increased. But it was also mentioned that with the increase in welding speed pitting potential was increasing. And at the speed of more than 2.5 mm/s, time required for redistribution of Cr and Ni was not available so passive layer stability decreased.[12]

M. Dadfar et. al. discussed the behavior of SS 316 L welded through GTAW, welding parameter was welding voltage 11±2 V, welding current 55 A, welding speed 1.16 mm/s and heat input was 0.518 KJ/mm. it was concluded that base metal of weldment has lower corrosion resistant. Fusion zone was acting as cathodic part.[13]

S.Samanta et. al. used an inter-pass temperature 150^0C and welded samples with a range of welding parameters, welding current 90-96 A, welding voltage 11-12 V and welding speed 0.63-0.74 mm/s. it was found that microstructure showed directionality near the fusion boundary but not at center. Depletion of Cr found at lower welding speed and at higher welding speed Cr formed scale and increased oxidation resistance.[14]

S. Kumar. et. al. used 6 mm thick sheet of AISI 304, AISI 305 and AISI 306 and samples were welded at welding speed 2.25, 3.03 and 3.84 mm/s, welding current and voltage was 120 A and 30 V. found that with increase in heat input, dendrite size and inter-dendrite spacing were increased and at low heat input maximum tensile strength and lower ductility found.[15]

X.Li. et. al. employed aging temperature 650 ^{0}C, welding speed was 0.33 mm/s to 0.83 mm/s with 70-100 A current and welding voltage was 11-12 V. It was discussed that aging temperature has no effect on weld metal matrix; it was austenitic with or without aging temperature. But as aging time was increased the precipitation at grain boundary was increased. And inter-granular corrosion was affected by aging time at 650 ^{0}C because of the agglomeration of $Cr_{23}C_6$ at grain boundary.[16]

A.Ravi Shankar et. al. got the sensitization because segregation of impurities at grain boundary, transpassive dissolution of passive film found. And structural change in the heat affected zone degrades the weldment strength, ductility and corrosion resistance, welded at 0.33 mm/s speed, 200 A current, 12.5 V and heat input was 1.5 KJ/mm.[17]

Oyetunji et.al. It was observed grain size variation of austenite in HAZ and sensitization was observed due to chromium carbide precipitation at grain boundary. In microstructure dark spots of inclusion were also observed under the welding speed of range 0.69, 1.25, and 2.63 mm/s, with power input of 12, 9.20 and 4.60 KW. An optimum hardness was found at high speed and at 9.20 KW power input.[18]

W. Chuiphan et. al. stated the observations that hardness and pitting potential was increased with the increase in welding speed, hardness of weld metal was less than the base metal and it was also observed that width of the weldment face and root was decreased with increasing welding speed. Welding speed was 1.5, 2.5 and 3.5 mm/s, welding current and welding voltage was 85 A, 95 A, 110 A, 15±1 V, 13±1 V and 11±1 V. Heat input was 0.85 KJ/mm,0.49 KJ/mm and 0.34 KJ/mm.[10]

Y. Lu. et. al. conclude that current density decreased with increase in heat input also found that acicular ferrite decreased and irregular ferrite were increased with increased heat input. Welding parameter was as following- welding speed 1.15 mm/s, 0.98 mm/s and 1.4 mm/s. welding currents were 106 A, 127 A and 180 A. welding voltages were 9 V, 10 V and 14 V where heat input was 0.83 KJ/mm, 1.30 KJ/mm and 1.80 KJ/mm.[19]

Formation of δ ferrite and change in microstructure at different inter-pass has no effect on micro-hardness at fusion zone. Different inter-pass temperature alters the formation of δ ferrite.[20]

2.8 LITERATURE GAP AND FORMULATION OF PROBLEM

On the basis of literature survey it can be said that weldments of stainless steel have corrosion issues, whether it was welded by Metal Inert Gas Welding (MIG) or Gas Tungsten Arc Welding (GTAW) or any other welding process. It was also witnessed that there was corrosion issues in thin samples as well as in thick samples. It was also noticed that autogenously welded samples and welded with filler material samples, both have corrosion problems.

Further, the welding parameter used for weldments to evaluate corrosion behavior, probably not giving the complete correlation between welding speeds and heat inputs. So there is a requirement of a wide range of welding parameters for better understanding to evaluate and correlate the corrosion behavior to welding speeds and heat inputs.

Hence an immense work has been going on in this field to understand corrosion behavior of stainless steel.

From the applications point of view, SS 316 has been selected for investigation with well designed welding parameters for welding 2 mm thin sheet of SS 316 by GTAW.

Following are the key objectives for current dissertation:

1. To design a set of welding parameters for welding the samples, this will give a wide range for better investigation.
2. Design of a sequence for different corrosion tests, this will give better understanding of corrosion behavior.
3. To study the microstructure of various weldments produced by different welding parameter.
4. Micro hardness test of all samples to see the effect of welding speeds and heat inputs.

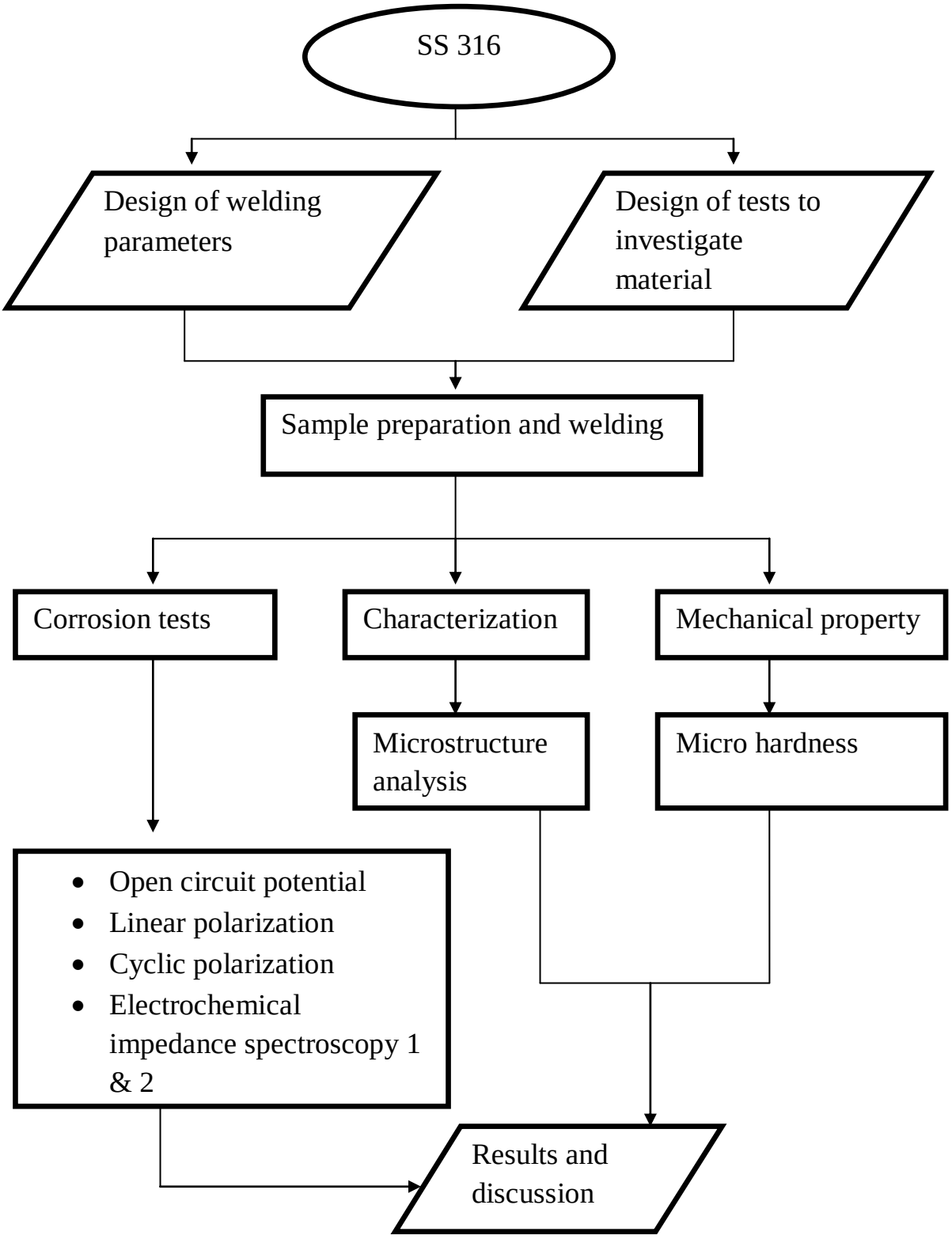

Fig.6 Flow diagram for plan of work

4.1 MATERIAL

SS 316 steel in the form of 2 mm thickness was used for the investigation during the experiments. Chemical composition is given in table below obtained by optical emission spectroscopy.

Table 1: Composition of SS 316

Material	Element wt%										
	C	Si	S	P	Mn	Ni	Cr	B	Cu	Mo	Fe
SS 316	0.05	0.42	0.002	0.014	1.34	11.07	17.54	0.0005	0.19	1.73	67.61

4.2 WELDING PROCEDURE

GTAW (Gas Tungsten Arc Welding) was used to join the SS 316 plates. It was an automatic machine.

Samples were fixed with the help of clamping unit in order to stop distortion caused by heat input. Tungsten inert gas torch was directed over specimen with the help of linear drive. The material investigated was SS 316 in the form of 2 mm thin sheet, so there was no further need of edge preparation. The weld was shielded with a pure argon gas at 10-12 L/min flow rate. Tungsten electrode with copper head and a cone angle of 30^0 and tip diameter of 3.2 mm was used. All the experiments were performed without filler metal with a gap of 0 mm between the metal sheets. Welding speed, current and voltage were systematically assorted to find suitable welding parameters. These experiments were approved with 1.4 mm distance between electrode tip and surface of specimen. A pre flow post flow was provided to purge the hoses and torch to protect the electrode from oxidation as they cool from welding temperature.

Fig.7 TIG welding machine Aristo ESAB modal LUD 450 W

4.2.1 SAMPLE PREPARATION FOR WELDING

Eighteen sheets of size 100 mm X 40 mm was taken out from 2 mm thick sheet of SS 316 to prepare nine samples using sheet cutter and hand hacksaw. Then edge preparation was done for square butt autogenous welds on a shaper machine.

Fig.8 Edge prepared sample for welding

4.2.2 WELDING PARAMETER

Following welding parameters were used for experiments. Listed below in Table 2

Table 2: Welding parameter used for joining

Sample name	Heat input (KJ/mm)	Welding speed(mm/s)	Voltage (V)	Current (A)
a1	0.80	1	9	90
a2	0.91	1	9.1	100
a3	1.10	1	9	123
b1	0.47	2	9.5	100
b2	0.86	2	12.2	142
b3	0.94	2	10.9	173
c1	0.43	3	10	123
c2	0.68	3	11.8	173
c3	0.81	3	11.6	212
Argon gas flow rate was 10-12 L/min				
Tungsten electrode used was 3.2 mm in diameter				

4.3 MICROSTRUCTARAL CHARATERIZATION

Samples obtained after welding were cut in to proper dimension and mounted with the help of molded epoxy. After mounting the samples every sample was first polished on belt polisher to flat the samples followed by paper polish though grit size 320, 800, 1200 and 1500. Samples were thoroughly washed after each polishing process to prevent scratch of abrasive particles.

For cloth polishing the samples, fine alumina (Al_2O_3) powder was mixed in to water to make a paste. And a wheel speed of around 280 rpm was used.

After polishing, all samples were etched with Aqua regia (1:3 HNO_3 and HCl) solution for 30 seconds and then swabbed with cotton.

Then all samples were examined with LEICA DMI 5000 optical microscope and microstructures were taken at different zones of welded samples.

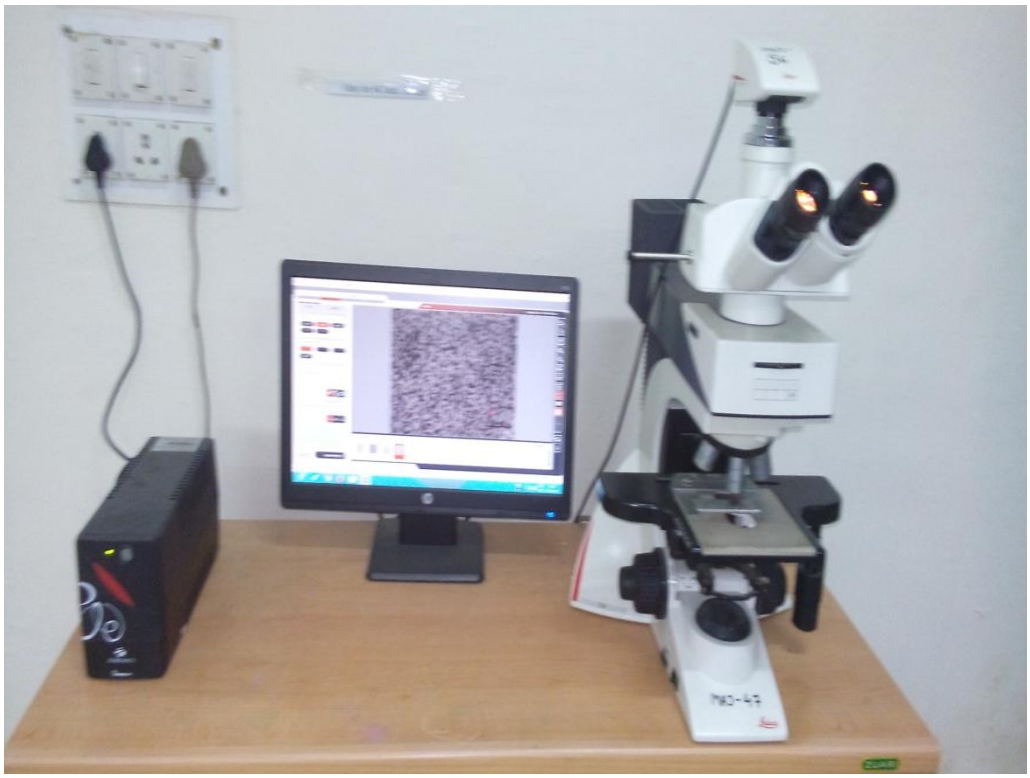

Fig.9 Leica DMI 5000 M optical microscope attached with digital camera

4.4 MICROHARDNESS

Hardness is a surface property defined as localized resistance of a material against deformation from the surface in the form of indentation, wear, cutting, scratch etc.

Microhardness of the samples were obtained using Vikers micro hardness tester Omnitech MVH-11.

First of all, samples were polished and etched then a load of 300 gm was applied with duel time 15 seconds and readings were taken at fusion, HAZ and base metal zone.

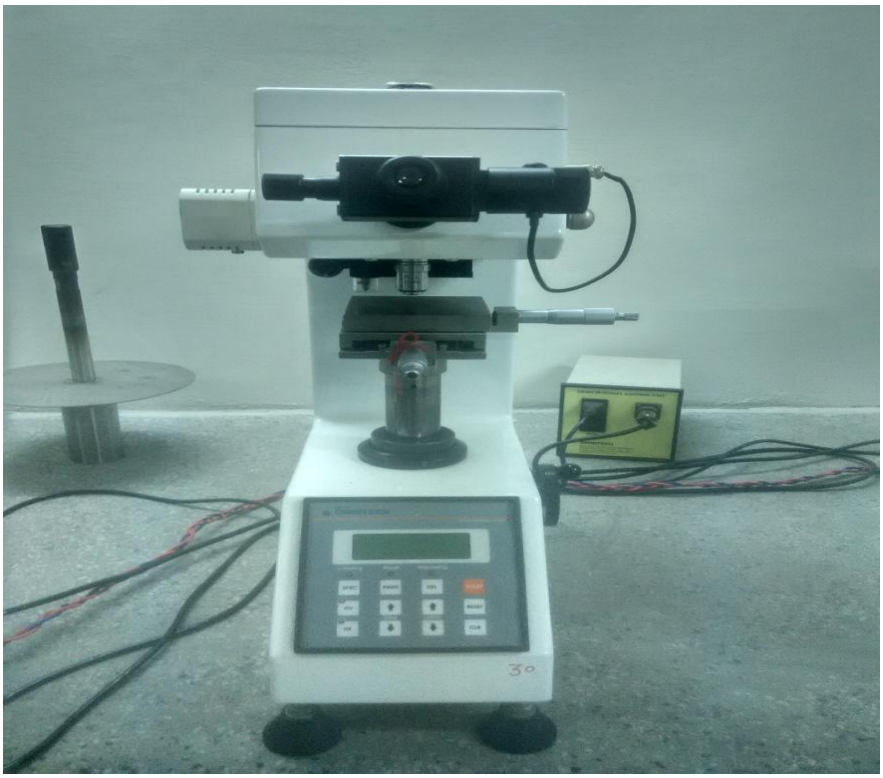

Fig.10 Vickers microhardness Tester Omnitech MVH-11

4.5 CORROSION TESTS

4.5.1 SAMPLE PREPARETION FOR CORROSION TEST

To study the corrosion behavior of welded SS 316, samples were prepared of fusion and heat affected zone using diamond cutter machine (Buehler Isomat 4000) for all welded joints prepared at different welding parameter and one base metal sample was prepared for comparison.

Every sample has to be mounted, so a thin conducting wire is welded at the back side of sample with the help of spot welding machine for the conducting purpose. After that samples were polished.

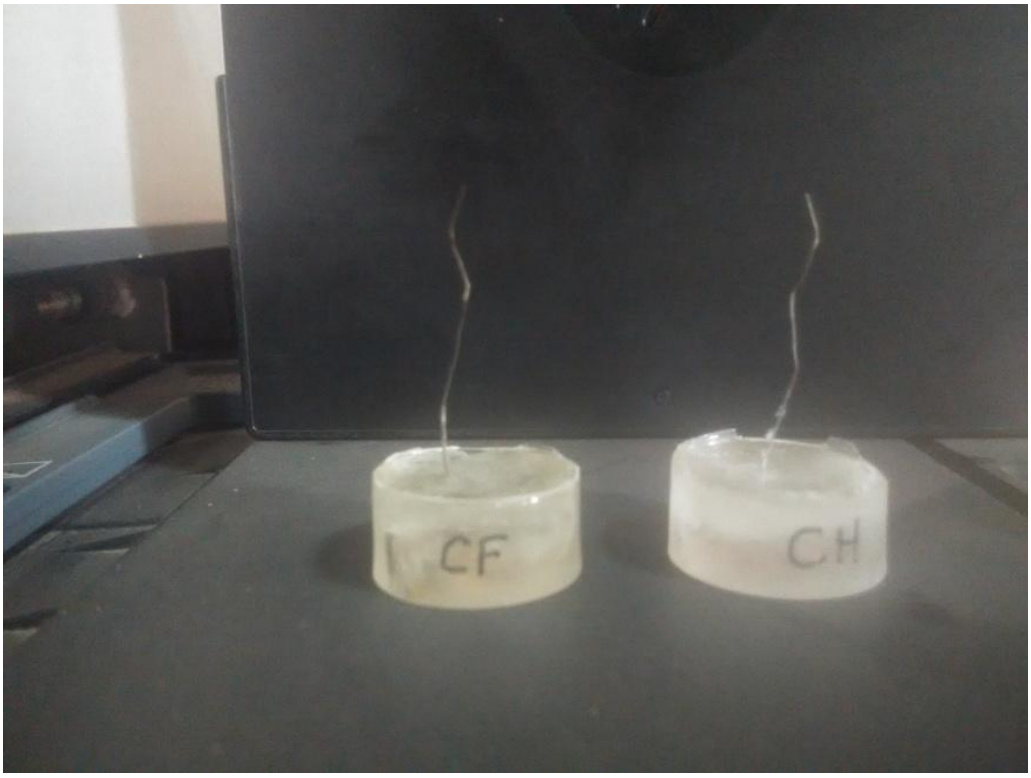

Fig.11 Mounted samples with conducting wire for corrosion test

Fig.12 Diamond cutter (Buehler Isomat 4000)

Fig.13 Spot welding machine

4.5.2 ELECTROCHEMICAL TESTS FOR CORROSION BEHAVIOR

To study the corrosion behavior of welded samples we have performed some electrochemical test on Potentiostat (Gamry Interface 1000) with flat cell is listed below:

- Open circuit potential test
- Linear polarization test
- Cyclic polarization test
- Electrochemical Impedance Spectroscopy (EIS) test

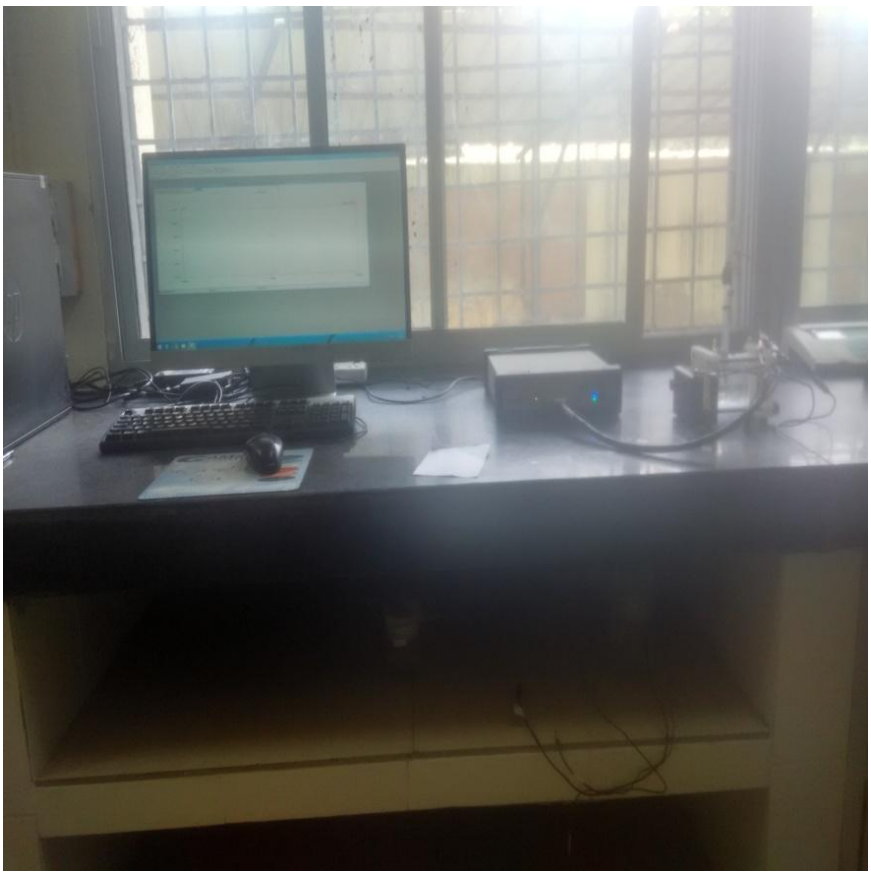

Fig.14 Potentiostat Gamry Interface 1000

4.5.3 OPEN CIRCUIT POTENTIAL

Open circuit potential tests were performed to know the behavior of all samples that, how they were stabilizing with time and achieving equilibrium potential.

Experimental set up used for test is listed below in table -

Table 3: Experimental set up for Open Circuit Potential

Electrolyte solution	3.5 wt% NaCl
Exposed sample area	20 mm^2
Total time (s)	3600
Sample period (s)	0.5

4.5.4 LINEAR POLARIZATION TEST

Linear polarization (polarization resistance) test is a non destructive test; it gives information without changing the surface condition of sample.

Experimental set up used for test is listed below in table -

Table 4: experimental setup for linear polarization

Electrolyte solution	3.5 wt% NaCl
Exposed sample area	20 mm^2
Initial E (V)	-0.02 vs E_{OC}
Final E (V)	0.02 vs E_{OC}
Scan rate (mV/s)	0.167

4.5.4 CYCLIC POLARIZATION

In cyclic polarization samples were polarized catholically and anodically in a cyclic manner to measure the pitting tendency of samples, it was a short time exposure test.

Experimental set up used for test is listed below in table -

Table 5: Experimental set up for cyclic polarization test

Electrolyte solution	3.5 wt% NaCl
Exposed sample area	20 mm^2
Initial E (V)	-0.25 vs E_{OC}
Final E (V)	0.25 vs E_{OC}
Apex E (V)	0.5
Apex I (mA/cm^2)	25
Forward scan (mV/s)	1
Reverse scan (mV/s)	1

4.5.5 ELECTROCHEMICAL IMPEDANCE SPECTROSCOPY TEST (EIS)

EIS is also a non destructive corrosion test uses very low voltage around 20 mV which is suitable for resistance and capacitance measurement by fitting the data in suitable model. We have done two EIS test, one is before corrosion and one is after corrosion.

Table 6: experimental set up for EIS test

Electrolyte solution	3.5 wt% NaCl
Exposed sample area	20 mm^2
Ac voltage (mV rms)	5
Initial frequency (Hz)	10000
Final frequency (Hz)	0.01
Apex I (mA/cm^2)	25
Forward scan (mV/s)	1
Reverse scan (mV/s)	1

5.1 WELD BEAD SHAPE

Weldments were prepared by different welding parameters and it was found that there was an incomplete penetration in the sample welded with parameter b1, and in sample c1 there was excess penetration.

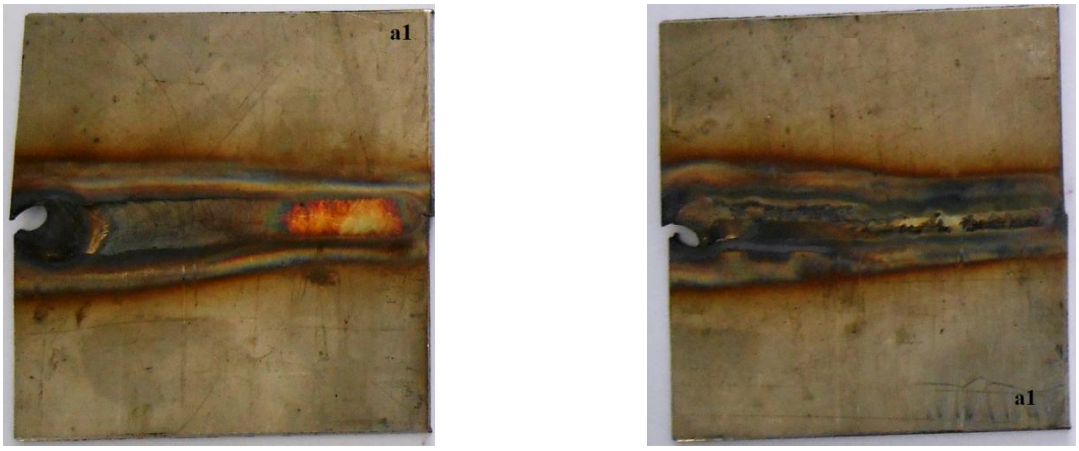

Fig.15 Weld bead shape of sample at face and root, welded at 1mm/s with low heat input

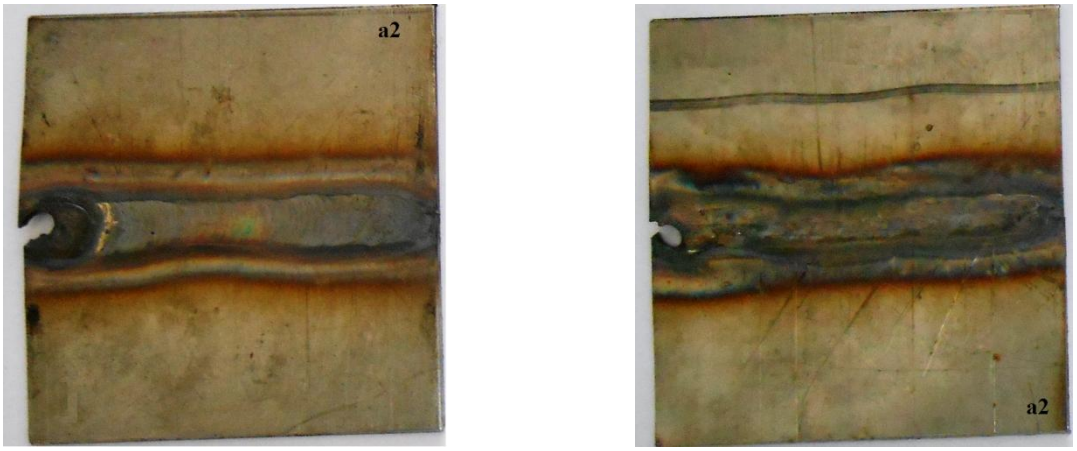

Fig.16 Weld bead shape of sample at face and root, welded at 1mm/s with medium heat input

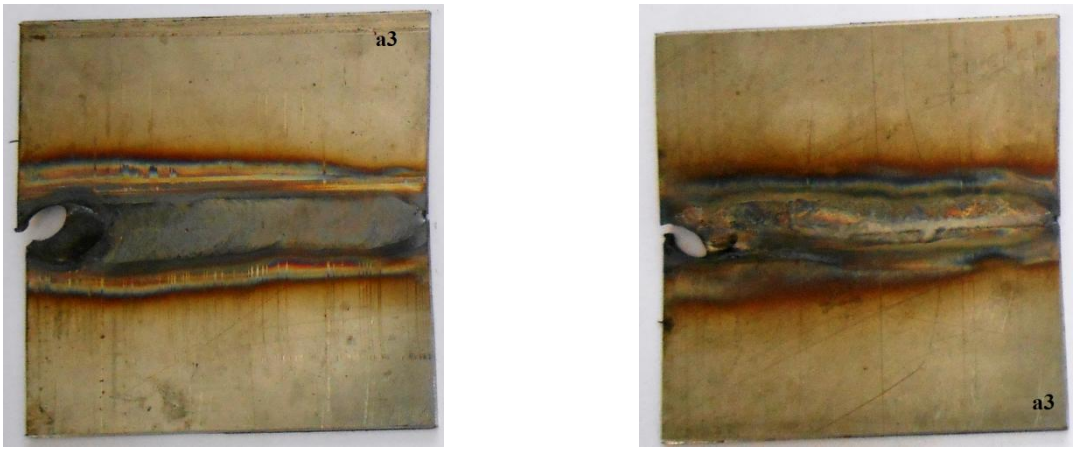

Fig. 17: Weld bead shape of sample at face and root, welded at 1mm/s with high heat input

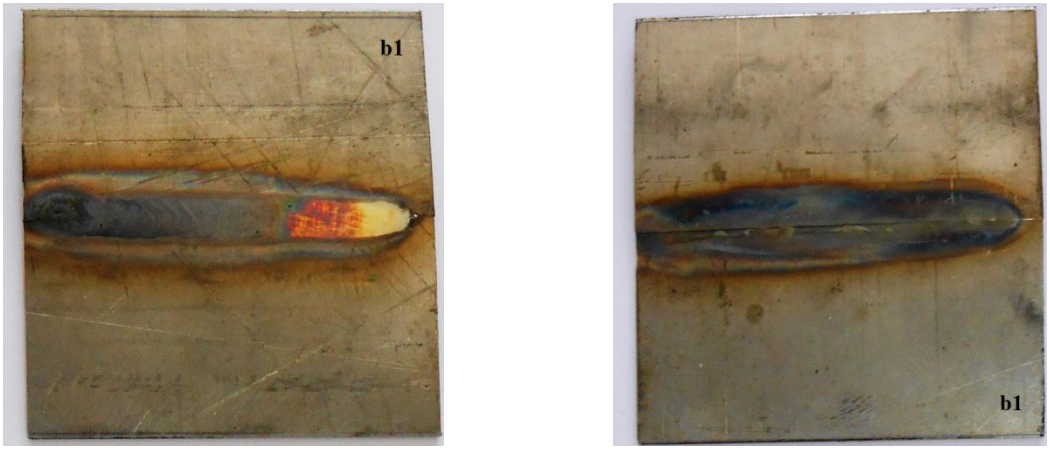

Fig.18 Weld bead shape of sample at face and root, welded at 2mm/s with low heat input

From the figures it can be noticed that at the same welding speed if the heat input was increased than there was a bead broadening at the face as well as at the root. This could be the reason that if the heat input is increased than there is sufficient time for cooling.

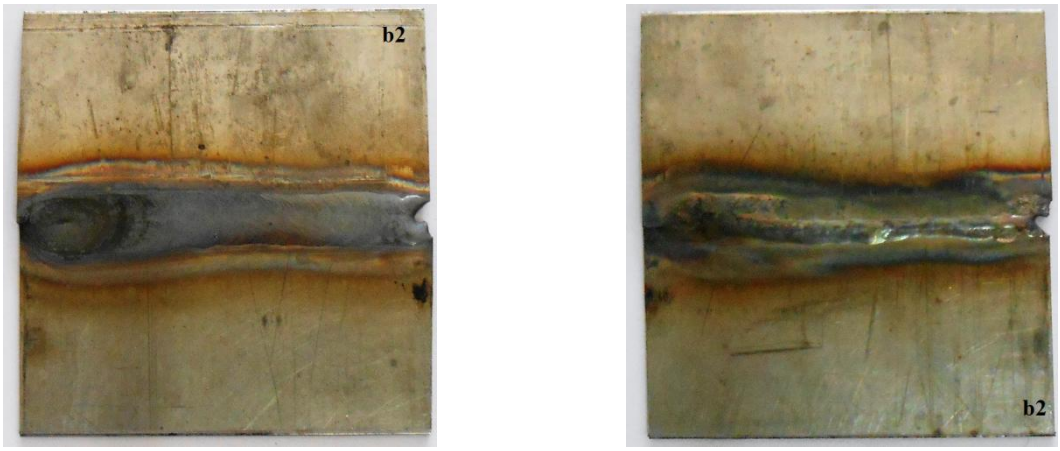

Fig.19 Weld bead shape of sample at face and root, welded at 2mm/s with medium heat input

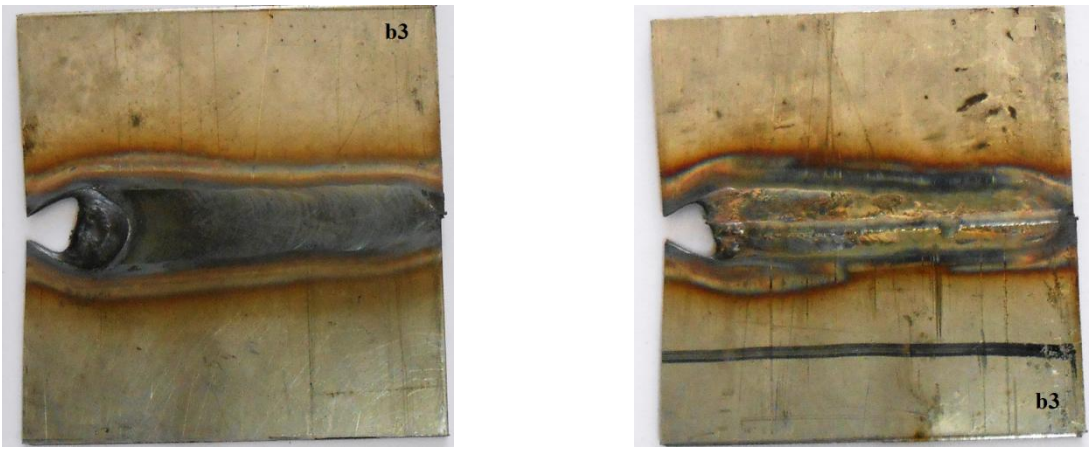

Fig.20 Weld bead shape of sample at face and root, welded at 2mm/s with high heat input

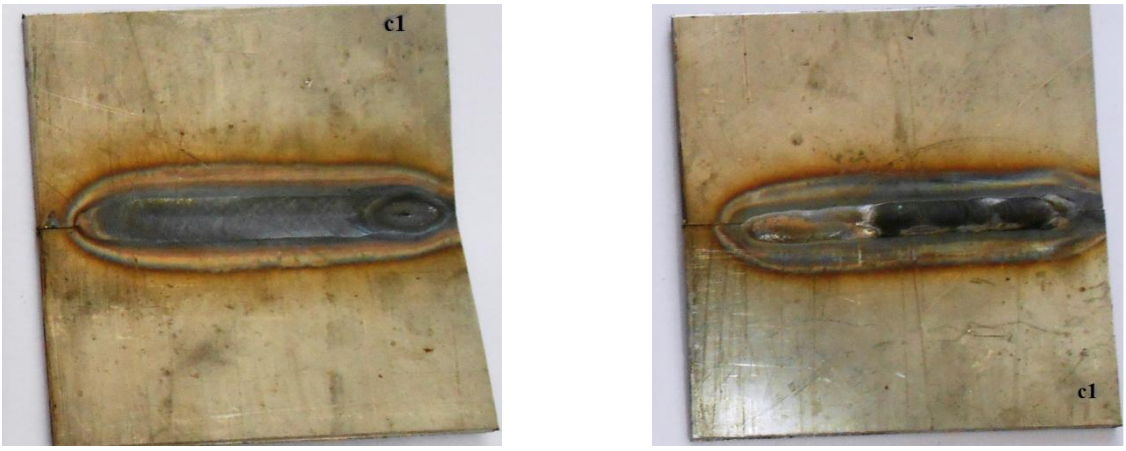

Fig.21 Weld bead shape of sample at face and root, welded at 3mm/s with low heat input

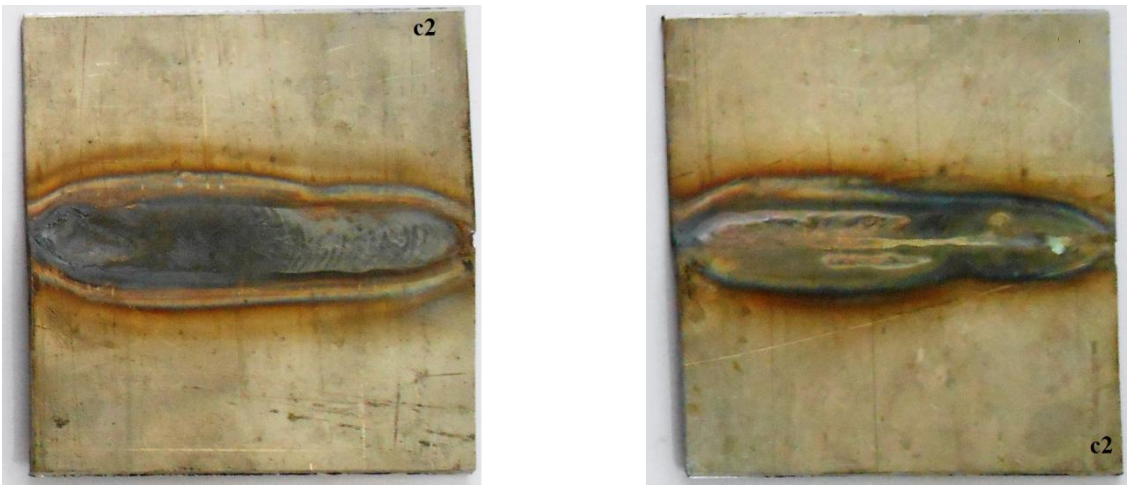

Fig.22 Weld bead shape of sample at face and root, welded at 3mm/s with medium heat input

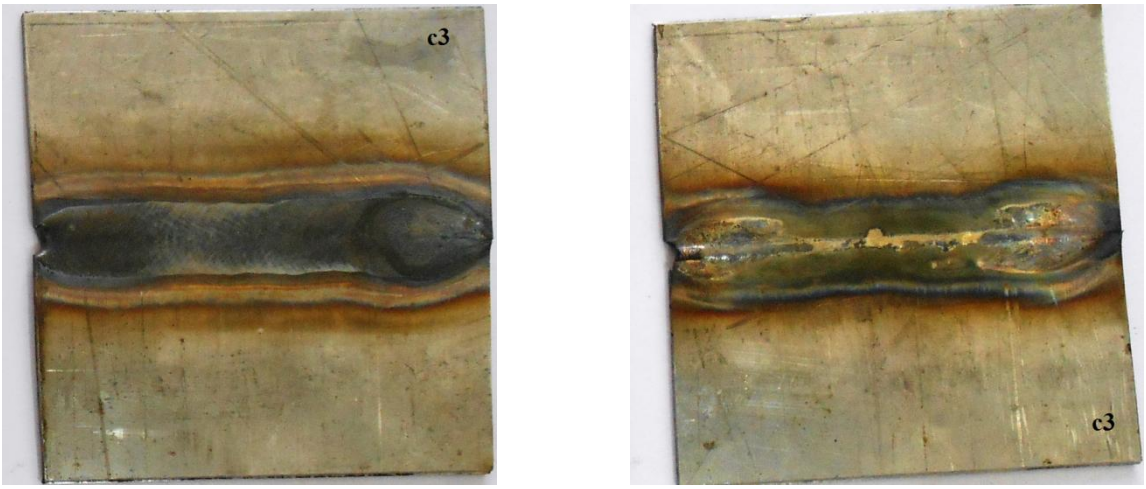

Fig.23 Weld bead shape of sample at face and root, welded at 3mm/s with high heat input

From the **Fig.** 20 it can be also notice that sample welded with parameter c1 shows excess penetration as well as bending of sample. Welding parameter c1 has highest speed and lowest heat input this could be the reason.

5.2 OPEN CIRCUIT POTENTIAL

Open circuit potential was evaluated for all samples; results are given in Fig. 13, 14 and 15. The behavior of samples welded at different welding parameters was evaluated in corrosive environment of electrolyte, 3.5 wt% NaCl by OCP measurement. In the fusion zone samples, higher potential values were measured for base metal, a1, a3, b2 and b3 and all other samples were showing lower potential values. In HAZ samples again base metal was showing highest potential value and b1, b3, c1 and c2 were showing potential near to base metal and others were showing lower potential values. From the results it can be said that samples having higher potential values has good corrosion resistance.

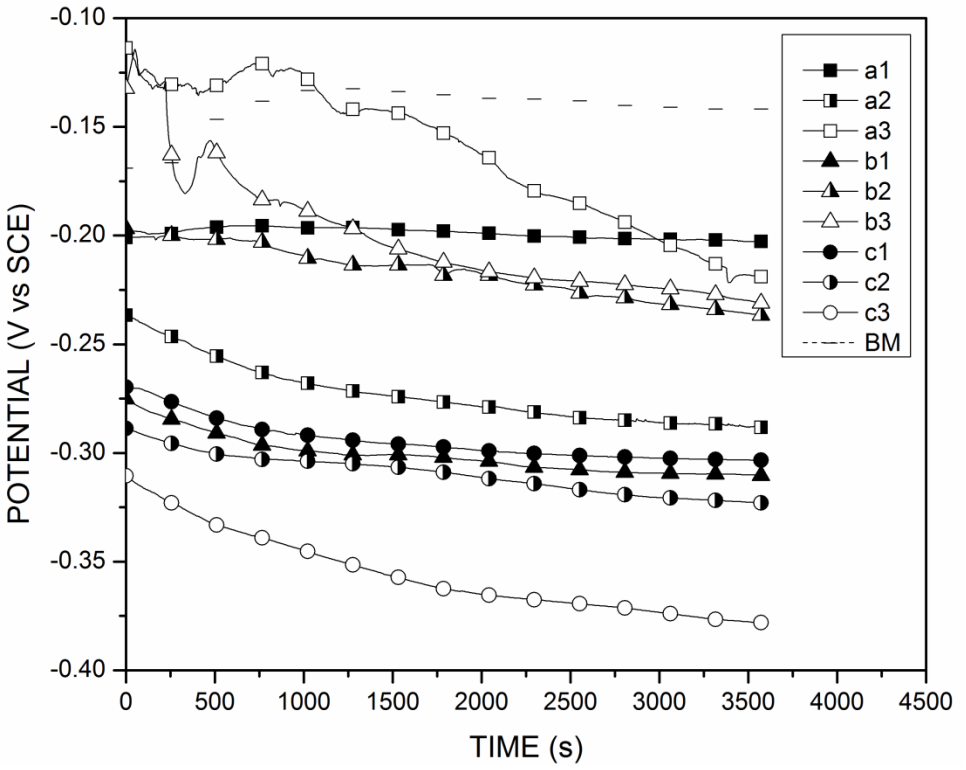

Fig.24 Open circuit potential graphs for all fusion zone samples with base metal

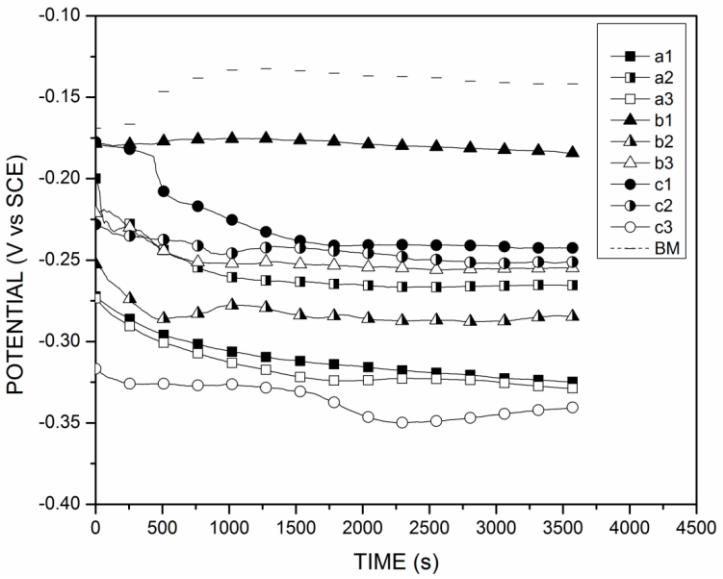

Fig.25 Open circuit potential graphs for all HAZ samples with base me

From the summary plot it can seen that among all the samples the potential difference between fusion zone and HAZ and between HAZ and base metal, sample b3 has lowest potential difference so there is a less chance of making galvanic couple as comparison to other samples. So we can say that welding parameter b3 is most appropriate.

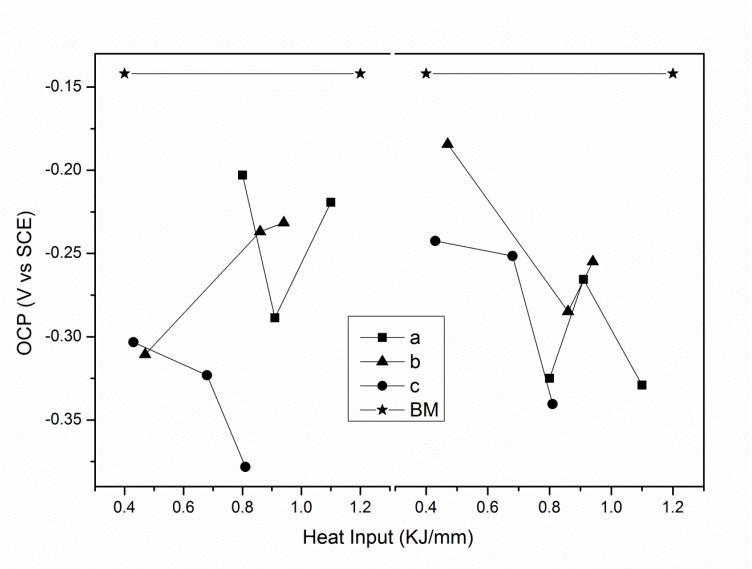

Fig.26 Summary plot (a) Open circuit potential Vs Heat input for fusion zone

(b) Open circuit potential Vs Heat input for HAZ

5.3 LINEAR POLARIZATION

Linear polarization results of all fusion and HAZ samples are presented in fig 16 and fig 17. From the plots it can be seen that slope of potential and current density near E_{corr} of a1, b2 and b3 are higher than other in fusion. Among fusion zone samples a3 and c3 showing lowest slope than others. Among HAZ samples b1, b3 and c2 showing larger slope than others.

From the summary plot it can be seen that polarization resistance (which is the slope of potential and current density at E_{corr}) of sample welded at speed 1mm/s (a) showing lower polarization resistance with increase in heat input. Same trend was obtained in sample welded at speed 3mm/s (c) in fusion zone. In HAZ samples no trend was obtained. Over all it can be concluded that sample welded at speed 2mm/s (b) with highest heat input value, giving polarization resistance better than other welding parameters.

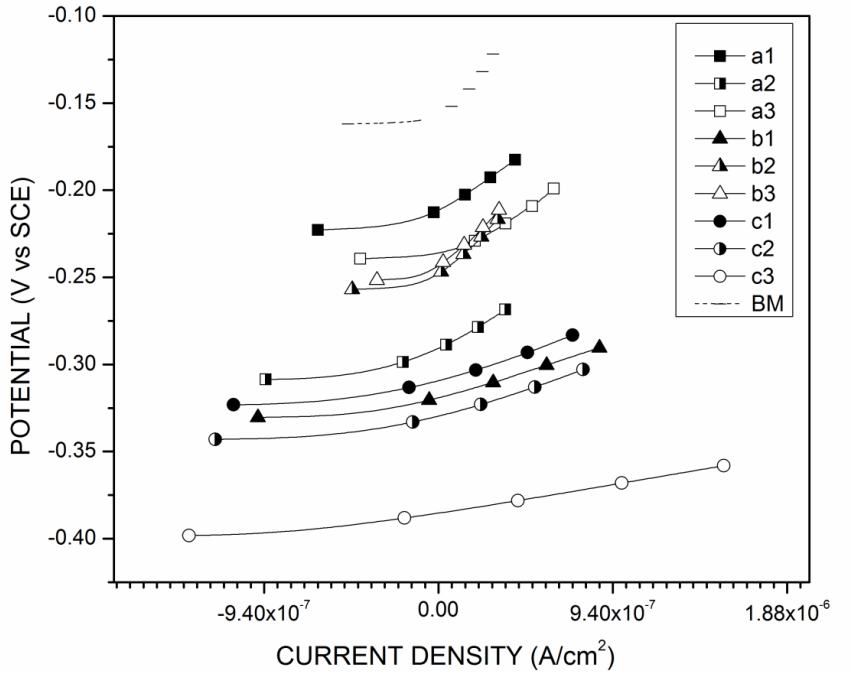

Fig.27 Linear polarization graphs for all fusion zone samples

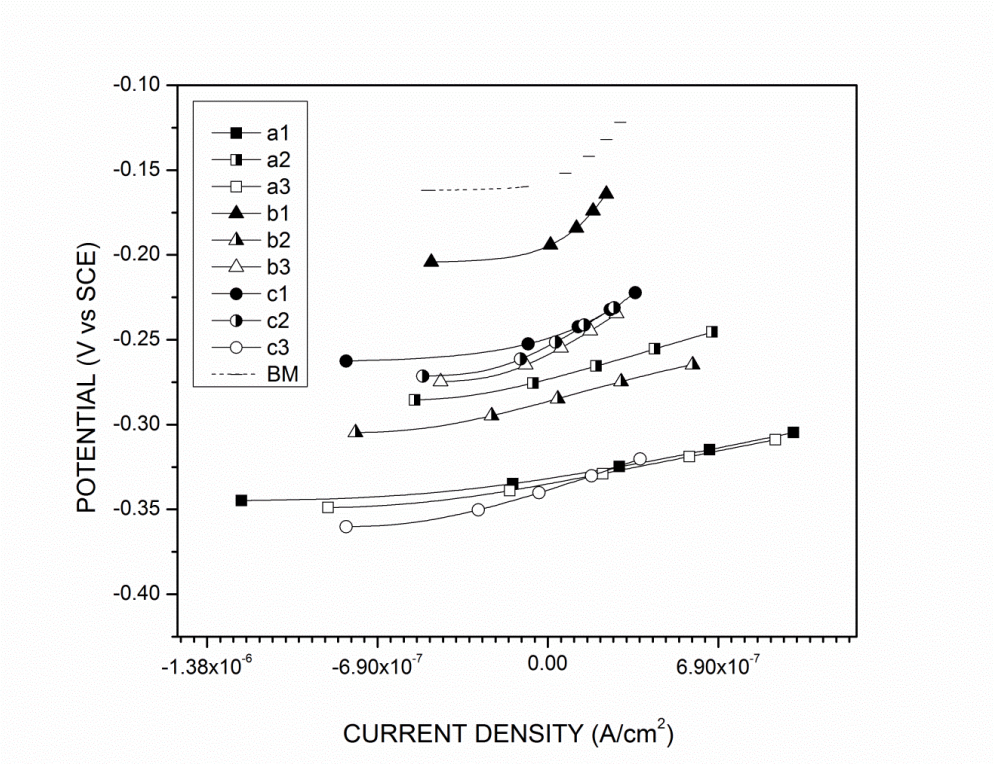

Fig.28 Linear polarization graphs for all HAZ samples

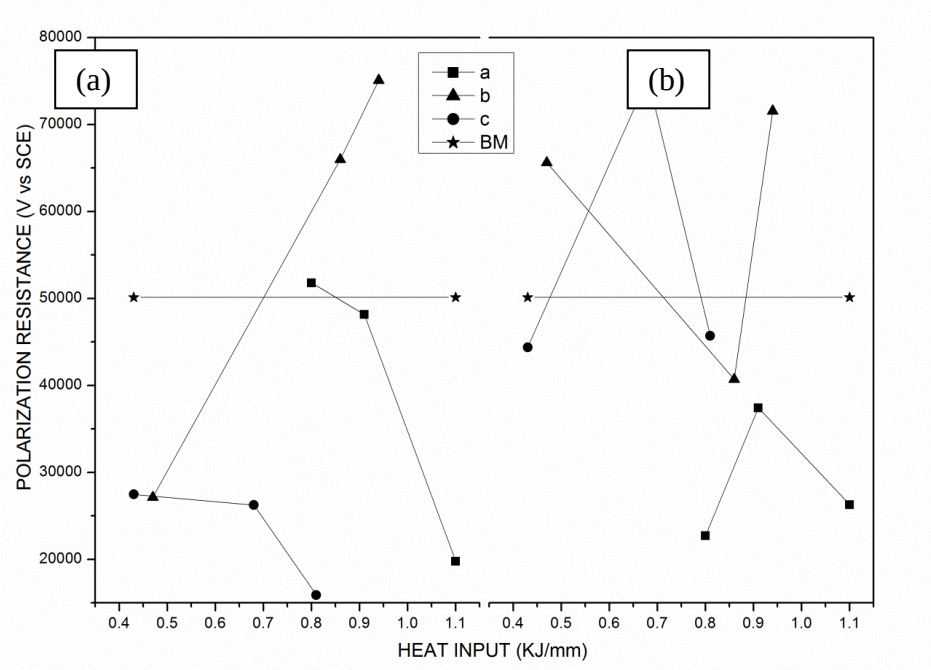

Fig.29 Summary plot (a) Polarization resistance Vs Heat input for fusion zone (b) for HAZ

5.4 CYCLIC POLARIZATION

Results obtained from cyclic polarization test are given in fig. 19,20 21 and 22. From the **Fig.** 19, 20, 21 and 22 it can be clearly seen that for all samples of fusion zone and HAZ, open circuit potential in the reverse scan has higher value than forward scan which indicates the formation of oxide film in the forward scan. Among all samples of fusion zone a2 and among HAZ c1 is showing largest difference between OCP of forward scan and reverse scan, but sample b3 has higher OCP in forward scan in fusion as well as HAZ as compare to other samples. It was also observed that difference between OCP values of fusion zone and HAZ for b3 was approximately zero, so there will be least chance for galvanic couple formation. Same conclusion was also observed in OCP test results. So it may be said that welding parameter b3 is best amongst other welding parameters.

From the figures it can also be seen that in fusion zone samples b3, a3 and base metal has higher pitting potential which reveals the pitting resistance ability, and a1, b1 and c2 showing lower pitting potential values which reveals less pitting resistance ability. In HAZ samples a3, c2 and a2 has higher value and c3, b2 and b3 has lower values of pitting potential.

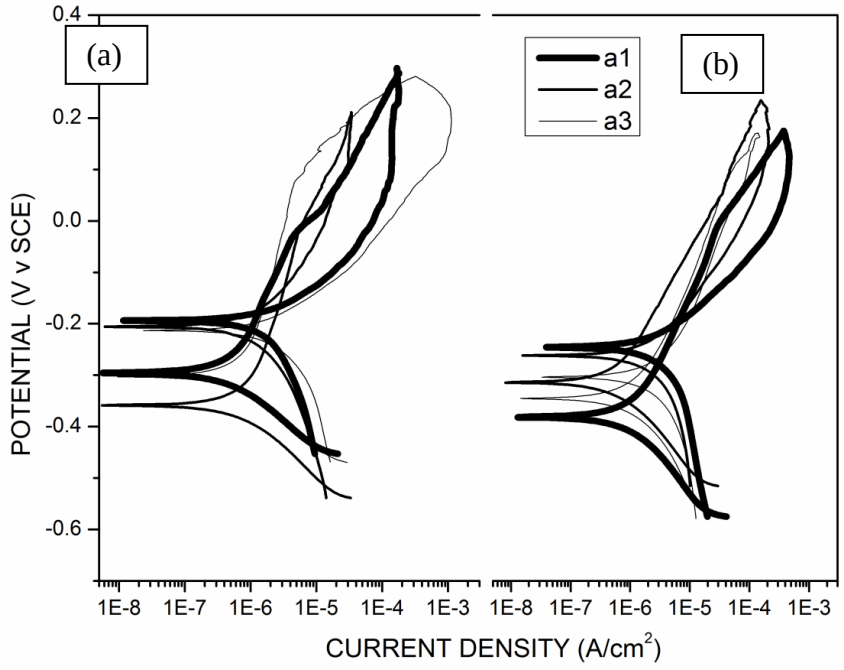

Fig.30 Cyclic polarization graphs of sample a1, a2, a3. (a) fusion zone (b) HAZ

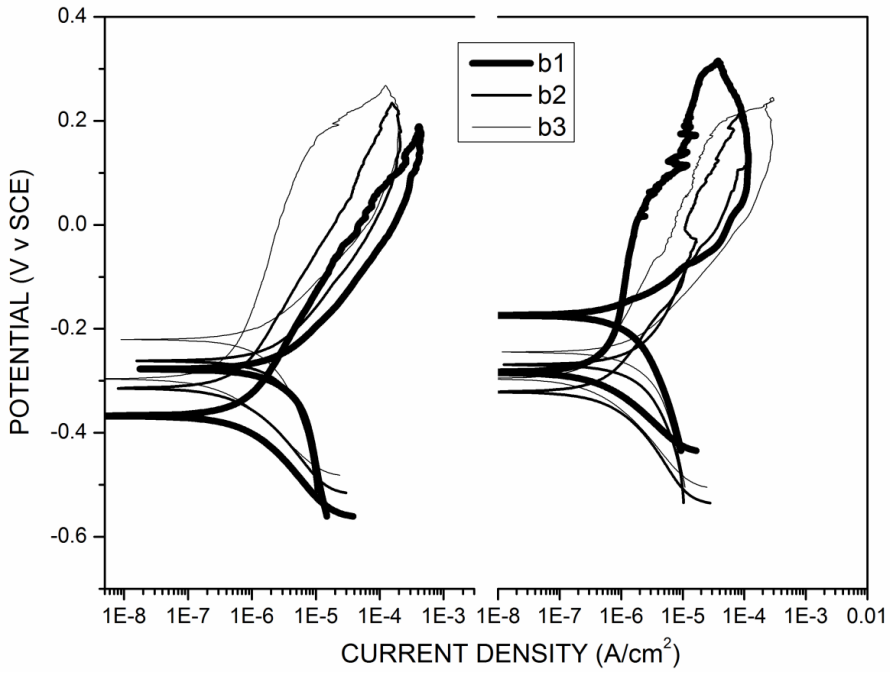

Fig.31 Cyclic polarization graphs of sample b1, b2, b3. (a) Fusion zone (b) HAZ

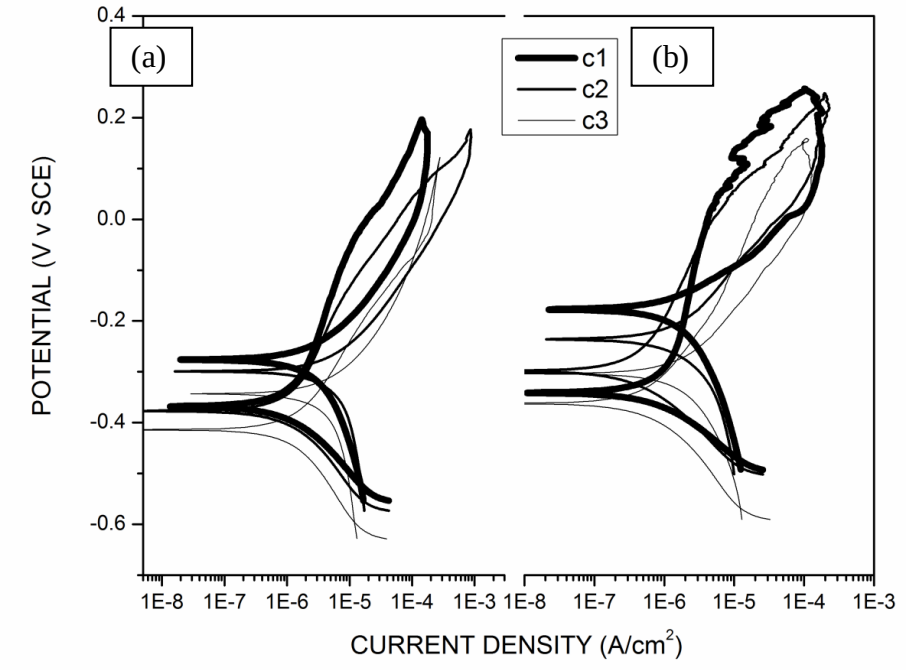

Fig.32 Cyclic polarization graphs of sample c1, c2, c3 (a) fusion zone (b) HAZ

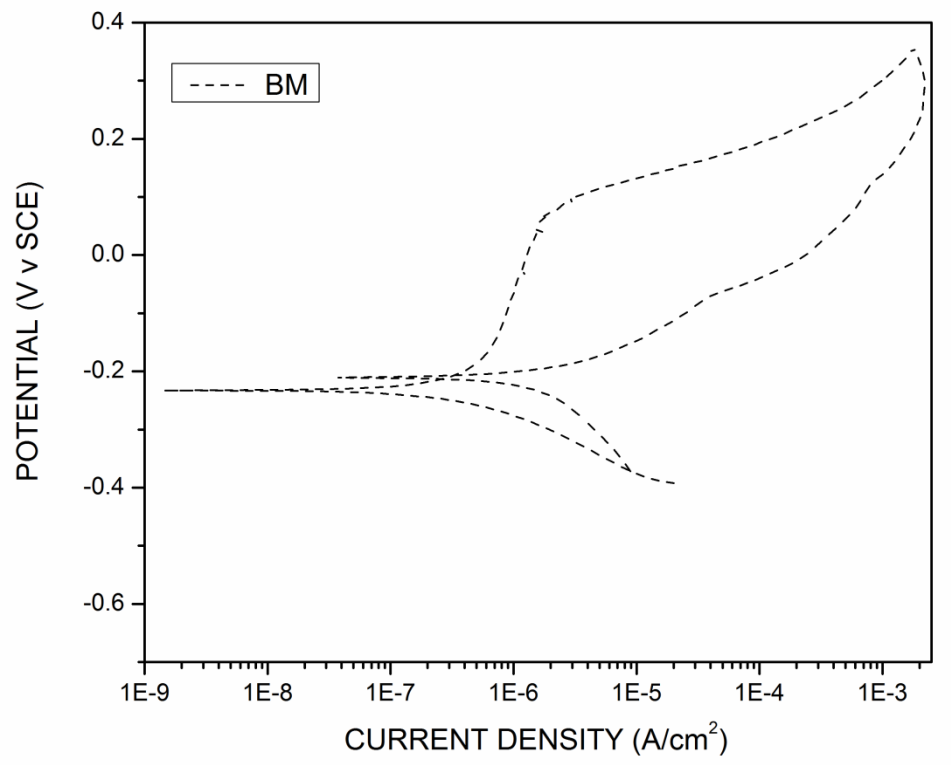

Fig.33 cyclic polarization graph of base metal sample

Repasive range in all samples can also be noticed from the cyclic polarization curves, curve which is showing more passive range can be assumed to perform well in corrosive environment. Here, amongst cyclic polarization curves obtained by fusion zone sample, welded at different welding parameters, b1, b3, a1, a2 and a3 has higher repassivation and in HAZ a1, b1, b2, c1 and c2 has higher repasive valuese range than others (**Fig.** 34) which shows sample can easily repassivate. Almost all samples showing some range

From summary plot (**Fig.** 35) it can observed that samples welded at different speeds, has lesser i corr with the increase in heat input value, in both fusion zone as well as HAZ and parameter b3 has the lowest i corr in both samples of fusion and HAZ, and it is also less than the base metal i corr .

So over all, after analyzing cyclic polarization curves of all samples of fusion zone and HAZ it can be said that welding parameter b3 is showing optimum performance.

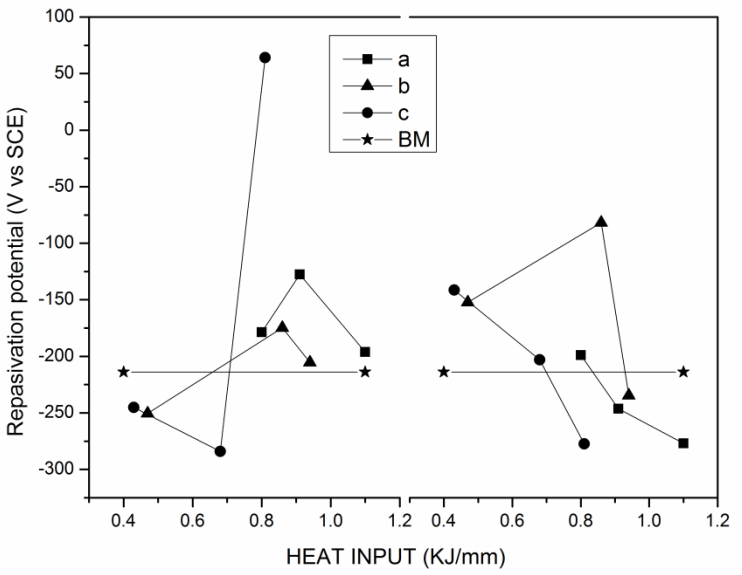

Fig.34 Summary plot: Repasivation potential Vs Heat input of samples welded at parameter a, b and c (a) for fusion zone (b) for HAZ

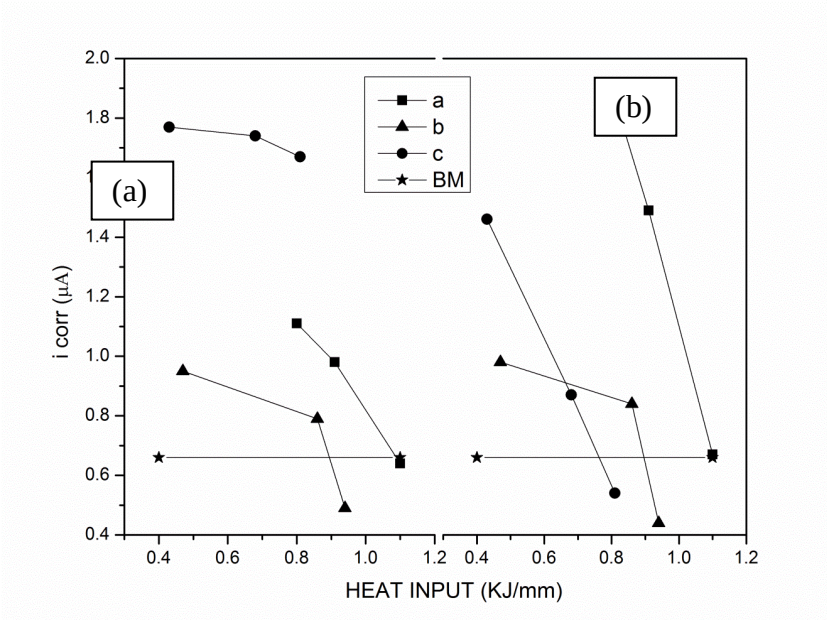

Fig.35 summary plot: i corr vs Heat input of samples welded at parameter a, b and c (a) for fusion zone (b) HAZ

5.5 ELECTROCHEMICAL IMPEDANCE SPECTROSCOPY (EIS)

EIS results obtained before linear and cyclic polarization test are given below –

Passive film of sample behaves like a dielectric and linearly varies the resulting impedance modulus logarithm. The penetration of electrolyte through pores and defects corresponds to loss of passive film properties. At the point where passive film lost, corrosion resistance and low frequency modulus decreases, this shows decrease in polarization resistance (R_p). In the **Fig.** 26 at fusion there is no variation with increased heat input but at HAZ there is a reduction in low frequency modulus, a1 is showing lowest value. It means between a1, a2 and a3 of HAZ a1 has less resistance to electrolyte.

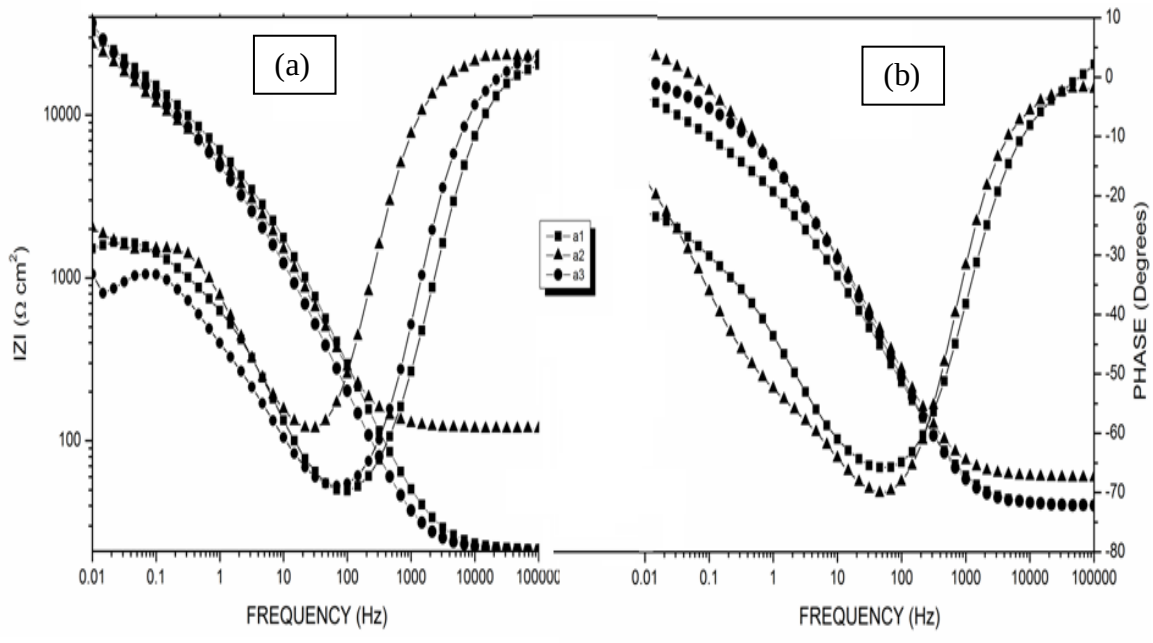

Fig.36 Bode, modulus and phase plots of sample a1, a2 and a3 (a) for fusion zone (b) for HAZ

In fig. 27 there is a variation in low frequency modulus at zones, fusion and HAZ. At fusion zone b1 is showing less value of low frequency modulus and b3 is showing larger value and in HAZ b2 is showing lesser value and b3 is showing higher value. On the whole b3 is showing good resistance to penetration.

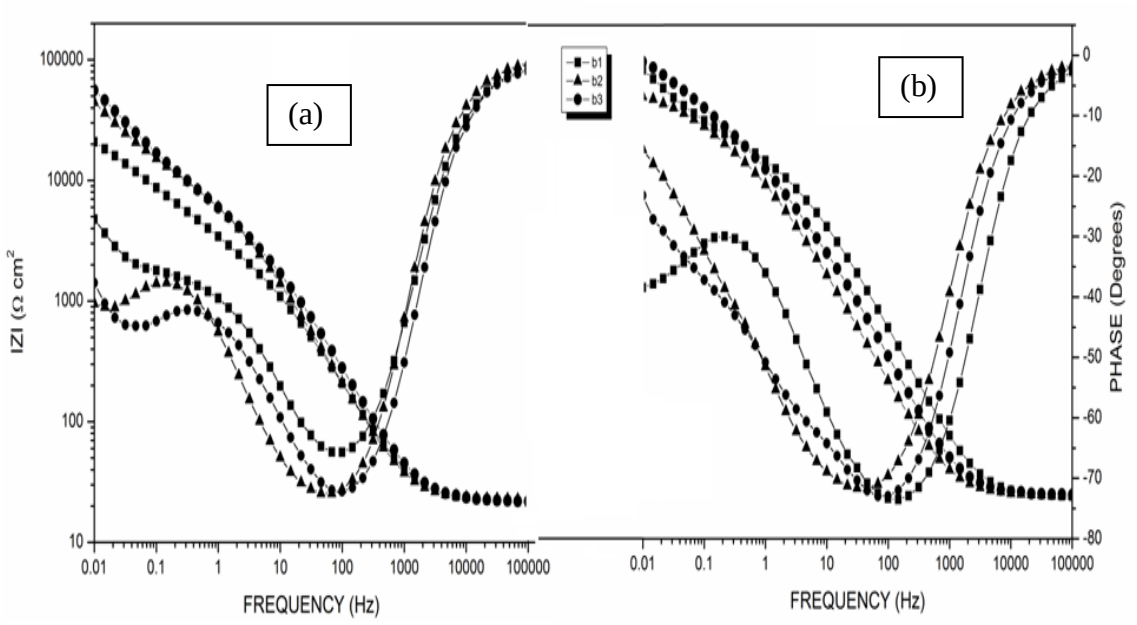

Fig.37 Bode, modulus and phase plots of sample b1, b2 and b3 (a) for fusion zone (b) for HAZ

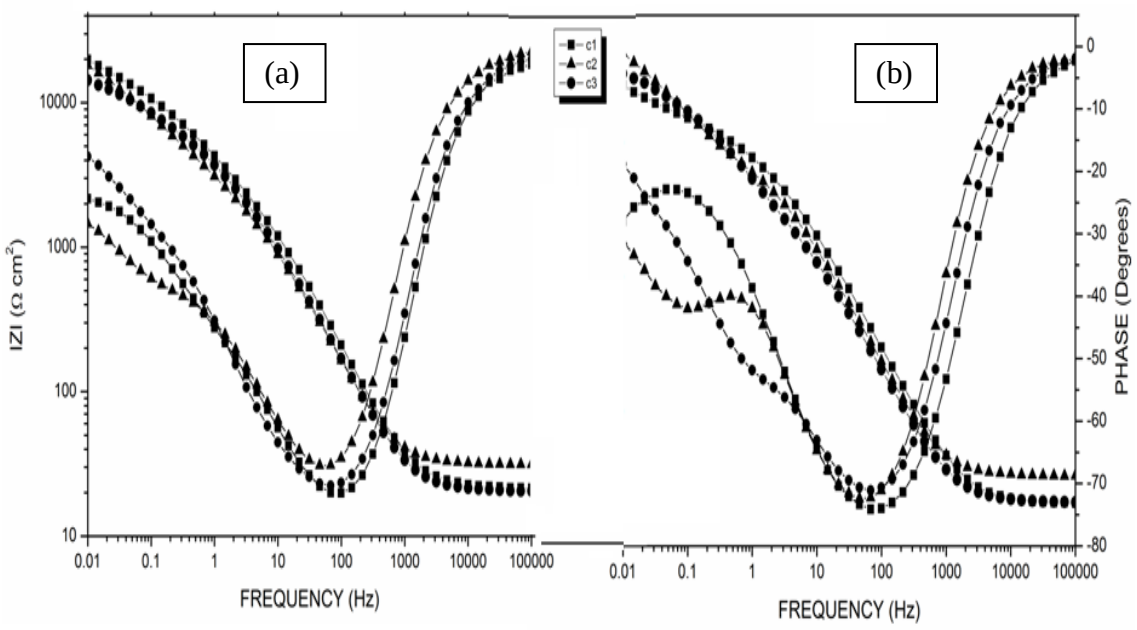

Fig.38 Bode, modulus and phase plots of sample c1, c2 and c3 (a) for fusion zone (b) for HAZ

In **Fig.** 28 there is no variation in low frequency modulus neither at fusion zone nor at HAZ.

EIS results obtained after linear and cyclic polarization test are given below –

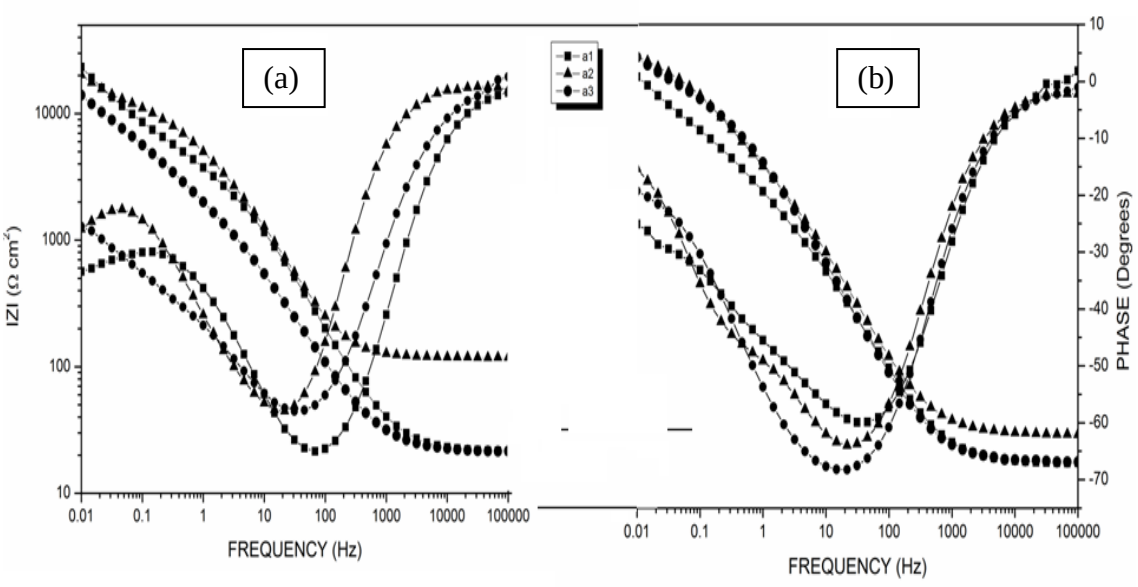

Fig.39 Bode, modulus and phase plots of sample a1, a2 and a3 (a) for fusion zone (b) for HAZ

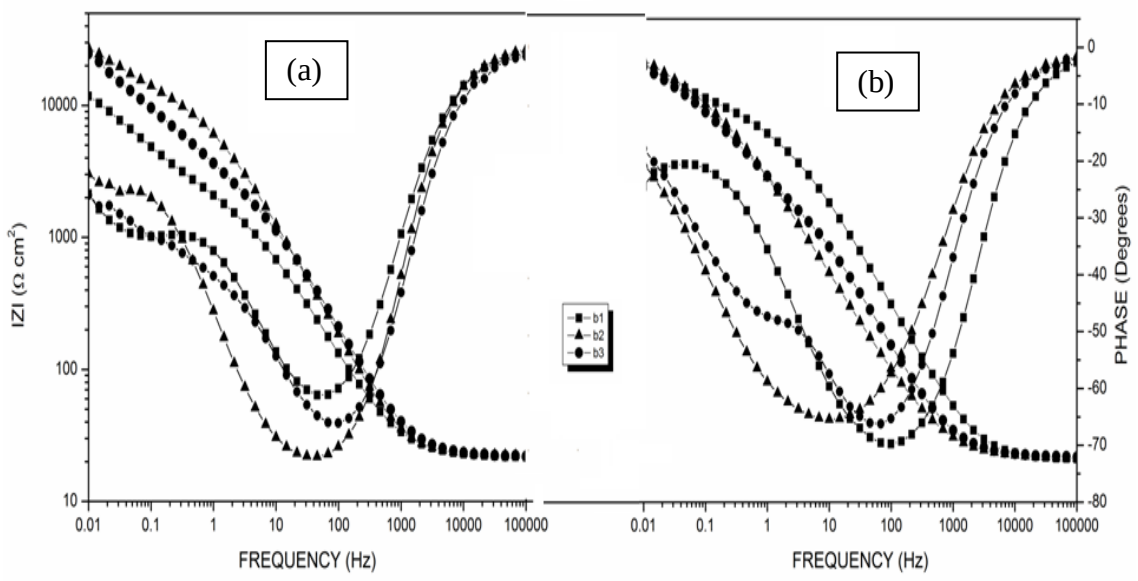

Fig.40 Bode, modulus and phase plots of sample b1, b2 and b3 (a) for fusion zone (b) for HAZ

From **Fig.** 29 it can be notice that at both zones fusion and HAZ there is a variation found, at fusion a3 has less low frequency modulus and at HAZ a1 has least. In fig. 30 b1 has least value at fusion zone and b2 has least value at HAZ.

In **Fig.** 31 at fusion zone c2 has least value and at HAZ all has approximately similar values. On the whole it can be said that EIS results obtained after polarization tests showing variations for all welding speeds, this notifies that there should be passive film loss in polarization tests.

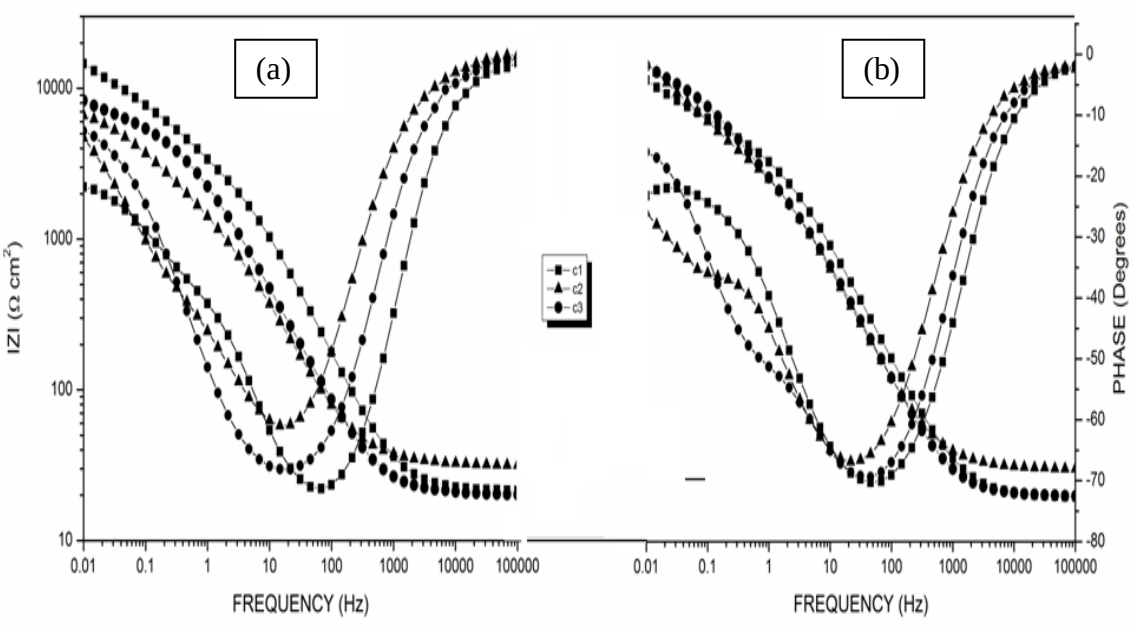

Fig.41 Bode, modulus and phase plots of sample c1, c2 and c3 (a) for fusion zone (b) for HAZ

Passive film resistance was measured with electrical equivalent circuit model by fitting imedence diagram shown in **Fig.** 32

Where, R.E. – reference electrode, W.E. – working electrode, Ru - solution resistance

Rp – polarization resistance, W_d – warburg impedence and Y_0 – admitance.

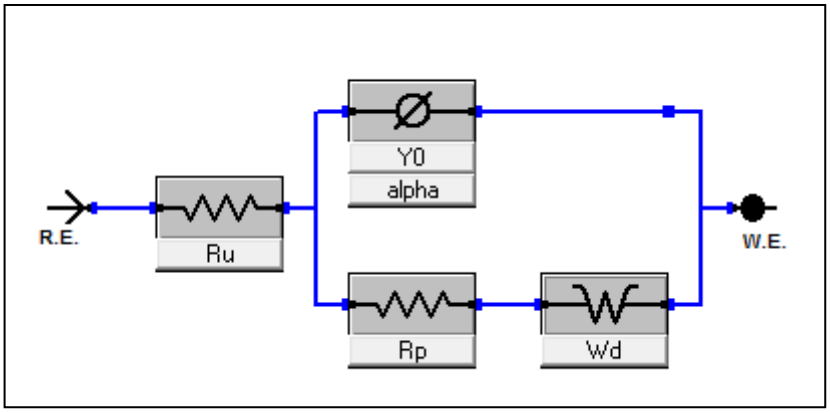

Fig.42 Electrical equivalent circuit at interface of passive film and electrolyte

Table 7: Data obtained by fitting the EIS 1 impedance to model.

EIS 1 (before polarization tests)					
Fusion zone					
Sample	Ru(Ω)	Y0 (S*s^α)	α	Wd (S*s^(1/2))	Rp (Ω)
a1	21.05	1.73E-05	8.26E-01	1.30E-04	7.49E+03
a2	116.4	2.11E-05	8.26E-01	1.66E-04	6.55E+03
a3	20.98	2.31E-05	8.41E-01	1.19E-04	5.52E+03
b1	21.25	2.80E-05	8.08E-01	1.92E-04	3.45E+03
b2	22.66	1.75E-05	8.76E-01	9.80E-05	5.96E+03
b3	20.82	2.74E-05	8.41E-01	3.32E-04	1.24E+04
c1	20.57	3.03E-05	8.00E-01	2.45E-04	7.21E+03
c2	30.47	3.63E-05	8.12E-01	2.25E-04	3.84E+03
c3	19.66	3.85E-05	7.96E-01	4.24E-04	6.97E+03
BM	19.99	1.19E-05	8.75E-01	9.55E-05	4.18E+03
HAZ					
a1	20.63	4.26E-05	7.88E-01	3.19E-04	6.76E+03
a2	31.73	3.28E-05	7.99E-01	1.89E-04	1.91E+04
a3	20.84	2.73E-05	8.42E-01	3.29E-04	1.24E+04
b1	21.07	8.51E-06	8.72E-01	9.86E-05	7.92E+03
b2	21.17	3.04E-05	8.26E-01	2.47E-04	1.60E+04
b3	21.35	1.85E-05	8.38E-01	8.52E-05	1.39E+04
c1	20.59	1.33E-05	8.62E-01	1.97E-04	1.06E+04
c2	33.53	1.28E-05	9.04E-01	8.68E-05	4.61E+03
c3	20.11	3.09E-05	8.00E-01	1.76E-04	1.63E+04

Table 8: Data obtained by fitting the EIS 2 impedance to model.

EIS 2 (after polarization tests)					
Fusion zone					
Sample	Ru(Ω)	Y0 ($S*s^{\wedge\alpha}$)	α	Wd ($S*s^{\wedge(1/2)}$)	Rp (Ω)
a1	21.43	2.51E-05	8.26E-01	1.99E-04	3.86E+03
a2	115.9	2.99E-05	7.98E-01	2.94E-04	8.92E+03
a3	20.86	8.74E-05	7.38E-01	3.42E-04	4.42E+03
b1	21.52	4.96E-05	7.89E-01	3.64E-04	2.30E+03
b2	22.07	2.31E-05	8.54E-01	2.07E-04	1.09E+04
b3	21.48	6.28E-05	8.07E-01	4.52E-04	9.59E+03
c1	20.89	3.43E-05	8.03E-01	3.48E-04	5.10E+03
c2	31.06	1.51E-04	7.18E-01	1.37E-03	4.47E+03
c3	20.06	8.50E-05	7.80E-01	1.44E-03	6.04E+03
BM	20.72	2.89E-05	8.10E-01	1.35E-04	3.88E+03
HAZ					
a1	20.43	9.43E-05	7.40E-01	4.06E-04	4.41E+03
a2	32.78	7.39E-05	7.46E-01	5.19E-04	1.24E+04
a3	21.48	6.28E-05	8.07E-01	4.52E-04	9.61E+03
b1	20.8	1.61E-05	8.22E-01	2.59E-04	9.09E+03
b2	21.69	7.64E-01	4.12E-04	1.86E+04	7.09E+03
b3	21.04	5.41E-05	7.54E-01	2.49E-04	8.49E+03
c1	20.74	2.42E-05	8.29E-01	2.96E-04	7.94E+03
c2	33.56	3.71E-05	8.20E-01	1.83E-04	6.23E+03
c3	20.42	4.71E-05	7.82E-01	3.27E-04	1.48E+04

5.6 MICROSTRUCTURE

The microstructure of solidified fusion zone and HAZ was observed of all the samples, welded at different welding parameters shown in fig. 31 to 39.

From **Fig.** (a) of 31, 34 and 37, the micrograph of samples of fusion zone (a1, a2 and a3), welded at same speed (1 mm/s) with increase in heat input. It can be observed from the micrographs that ferrite lathes are interconnected and coarsening has been observed with increase in heat input. It may be the region that at low heat input, cooling rate is fast so there is not enough time for transformation of ferrite to austenite therefore some delta ferrite remained in the austenite matrix at room temperature.

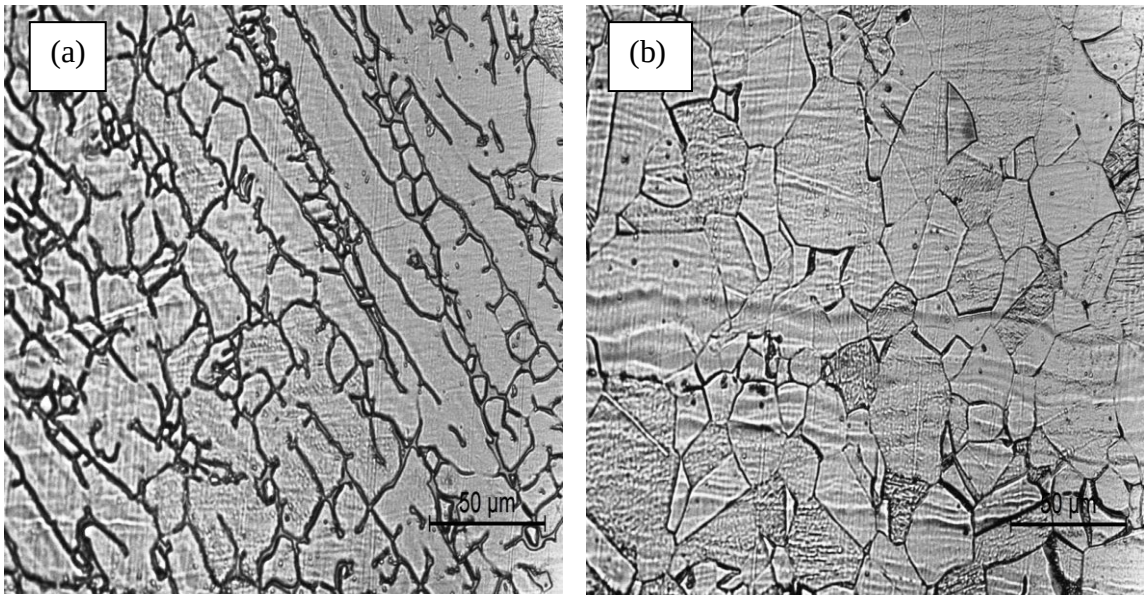

Fig.43 Microstructure of sample a1 (a) at fusion zone (b at) HAZ

From **Fig.** (a) of 32, 35 and 38, micrograph of samples of fusion zone (b1, b2 and b3) welded at speed 2 mm/s with increase in heat input showing the same trend as observed in sample a1, a2 and a3. Samples welded at speed 3 mm/s with increase in heat input also showing same trend and reasoning may be the same.

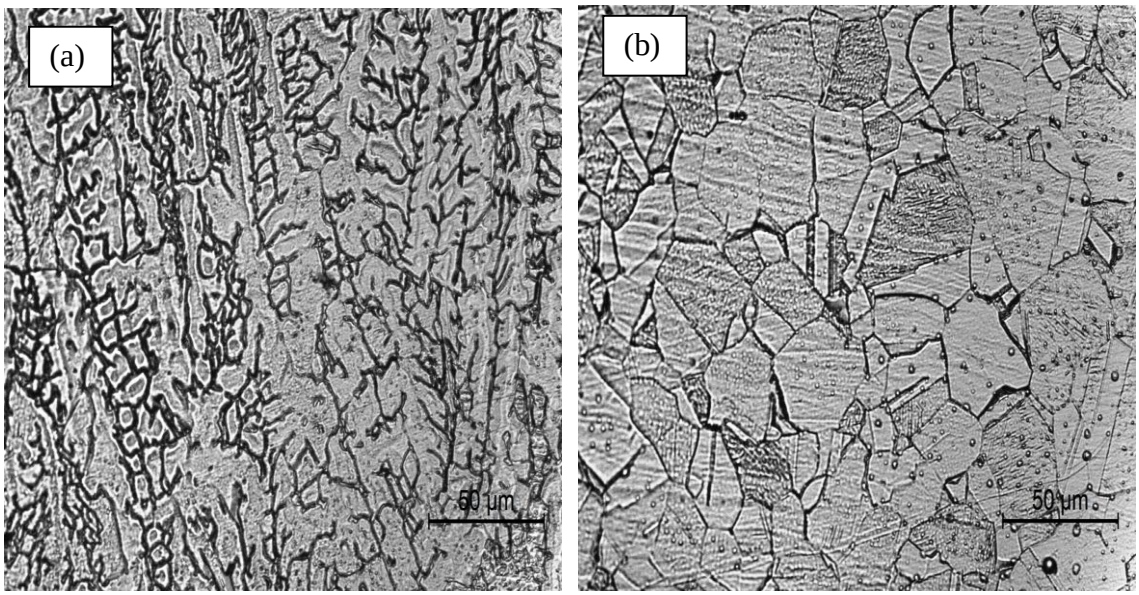

Fig.44 Microstructure of sample b1 (a) at fusion zone (b) at HAZ

It can be also seen in the **Fig.** 31 to 39 that dendrite size and direction is changing with the change in welding speed and heat input. Most likely the region was different cooling rate. The samples with high welding speed and low heat input has less cooling time and because of this delta ferrite dendrites are finer and have less inter dendrite space.

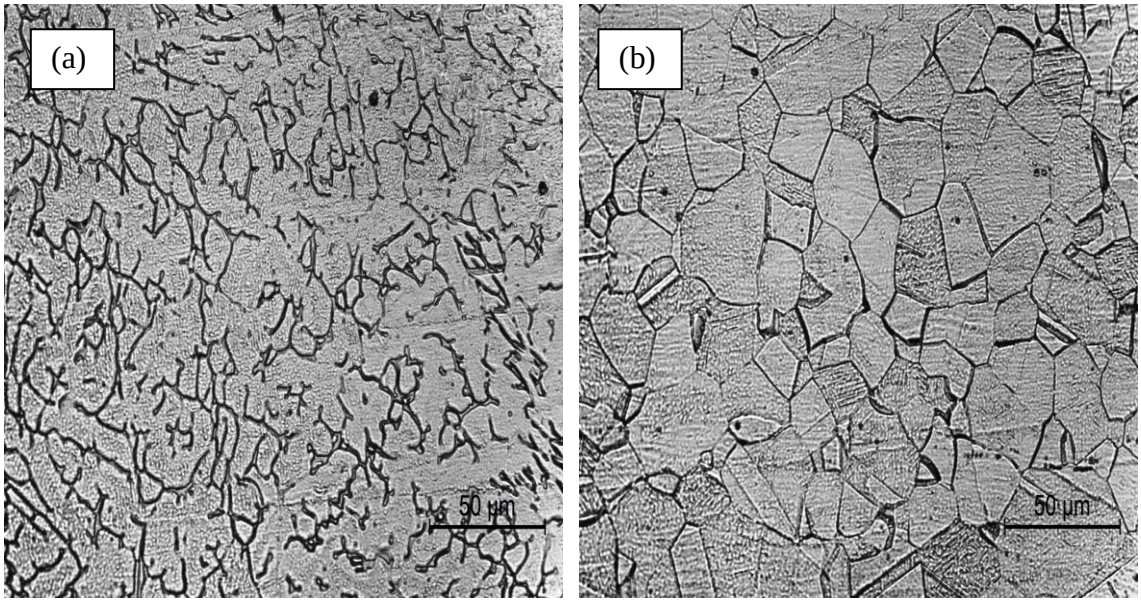

Fig.45 microstructure of sample c1 (a) at fusion zone (b) at HAZ

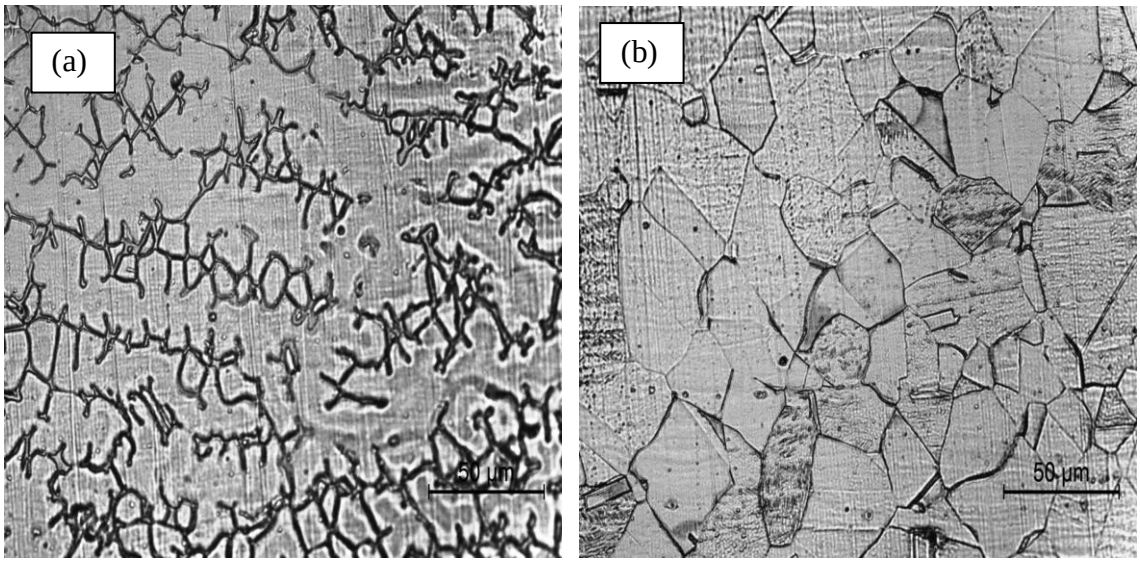

Fig.46 microstructure of sample a2 (a) at fusion zone (b) at HAZ

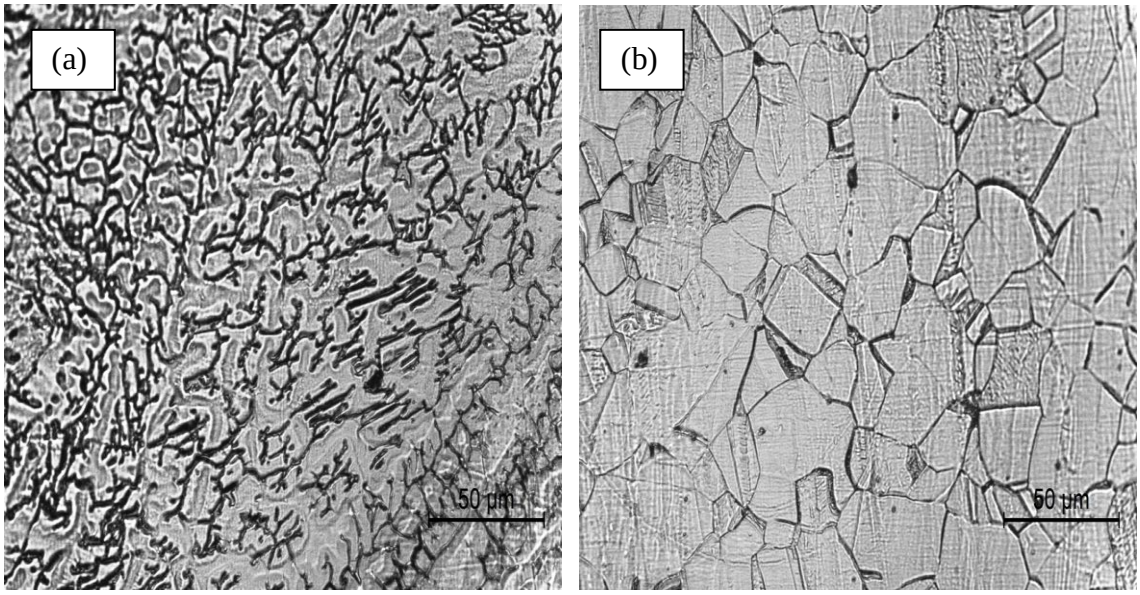

Fig.47 microstructure of sample b2 (a) at fusion zone (b) at HAZ

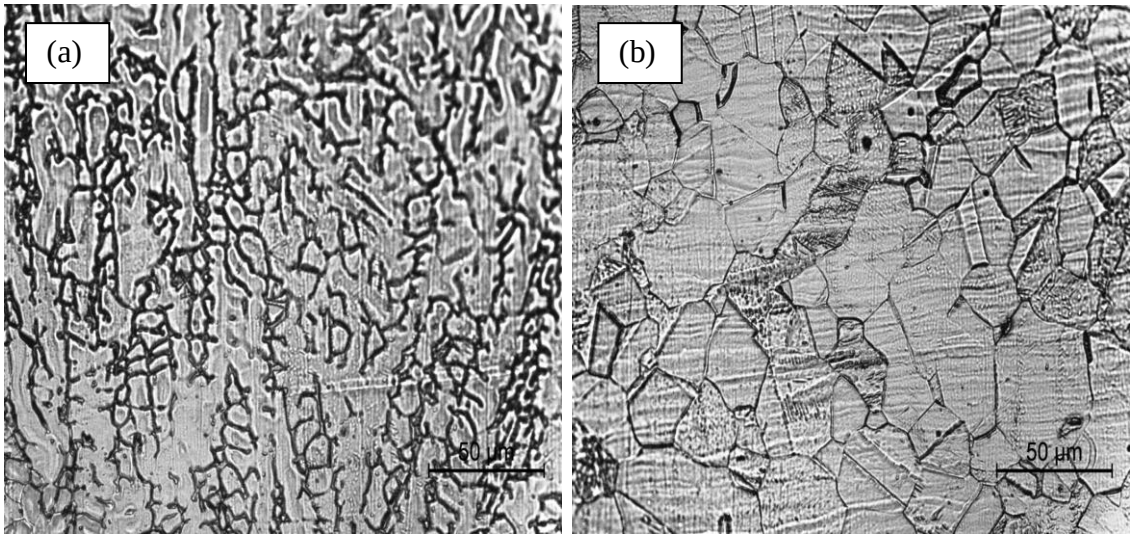

Fig.48 Microstructure of sample c2 (a) at fusion zone (b) at HAZ

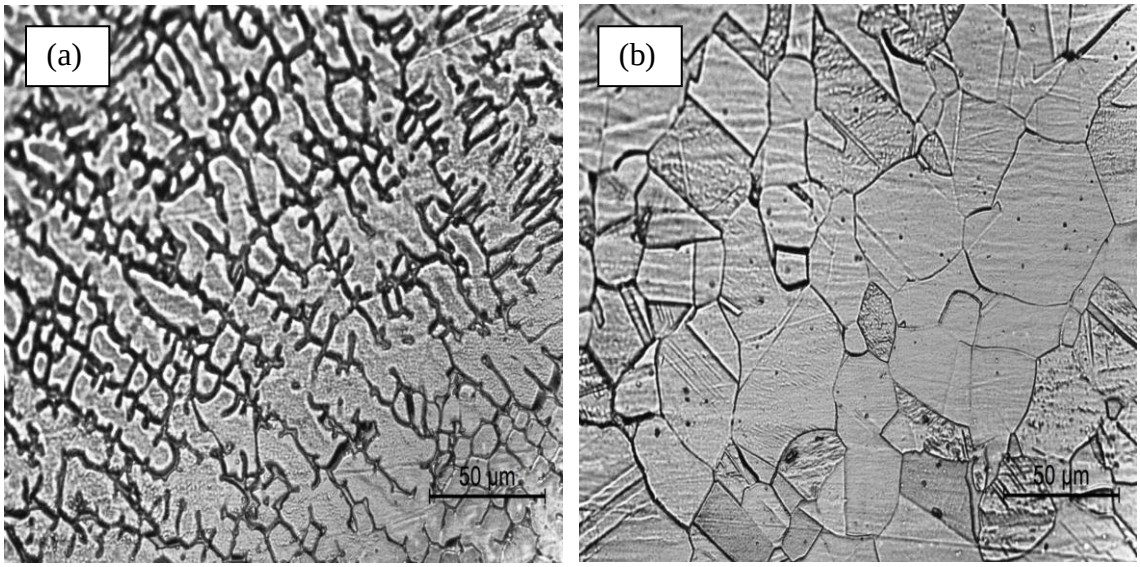

Fig.49 Microstructure of sample a3 (a) at fusion zone (b) at HAZ

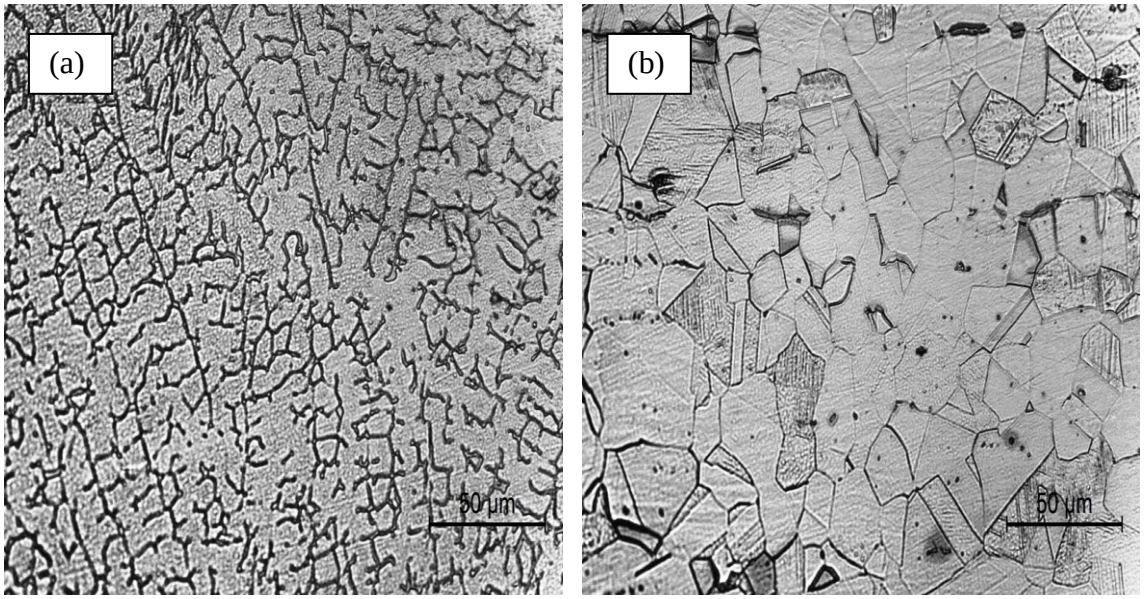

Fig.50 Microstructure of sample b3 (a) at fusion zone (b) at HAZ

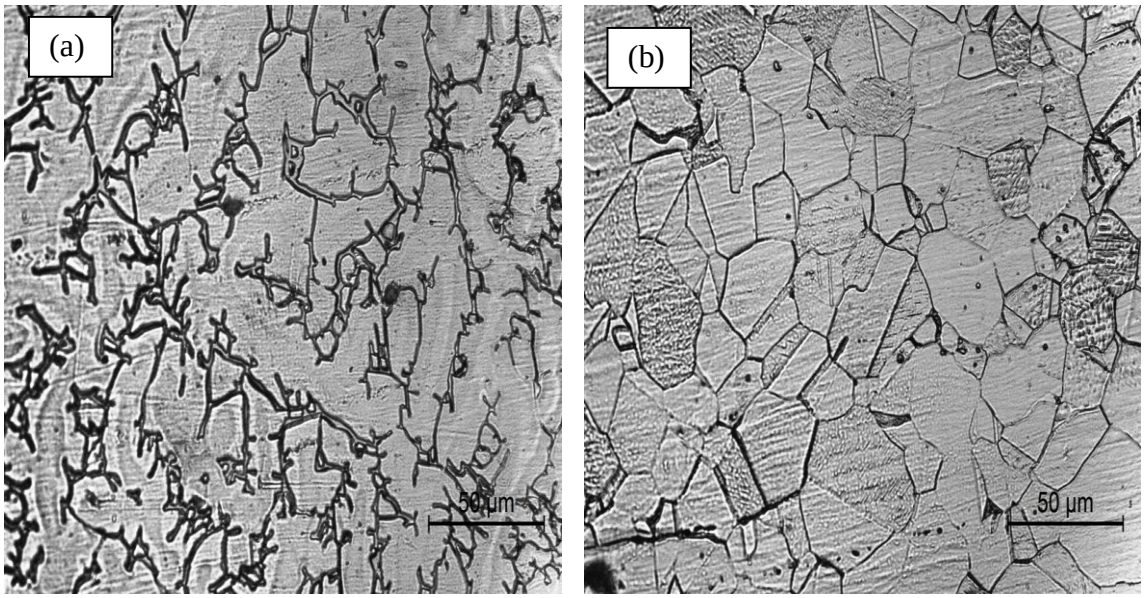

Fig.51 Microstructure of sample c3 (a) at fusion zone (b) at HAZ

5.6.1 MICROSTRUCTURAL ANALYSIS FOR DELTA FERRITE

It can be seen from the figures below that delta ferrite content is decreasing with the increase in heat input. It may the reason that at low heat input there is less time for cooling so transformation from delta ferrite to austenite is low, with high heat input there is sufficient time for transformation so delta ferrite content is less.

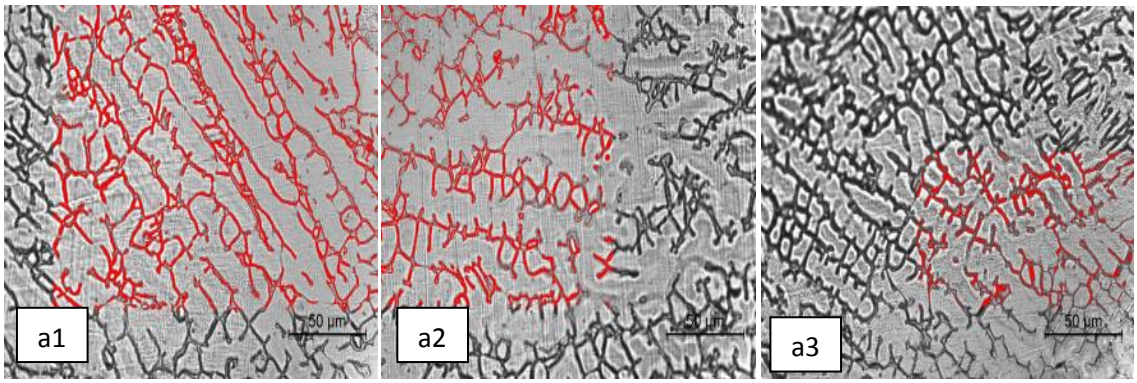

Fig.52 Delta ferrite dendrites of sample a1, a2 and a3

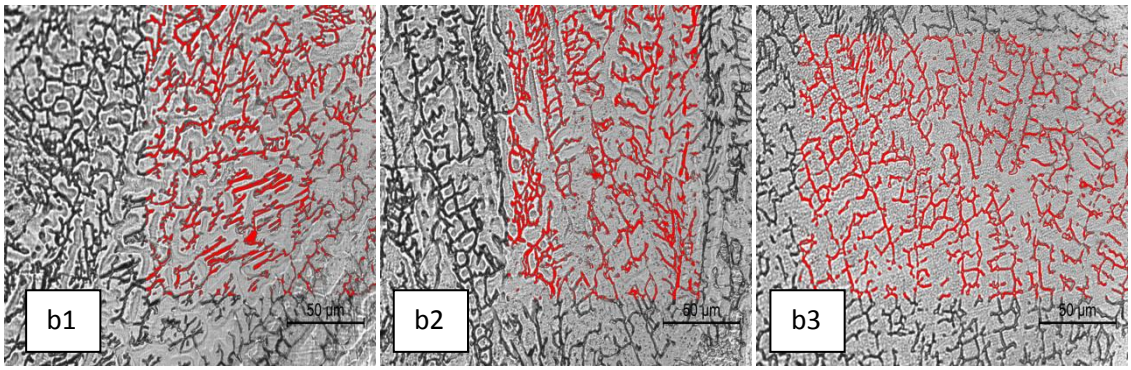

Fig.53 Delta ferrite dendrites of sample b1, b2 and b3

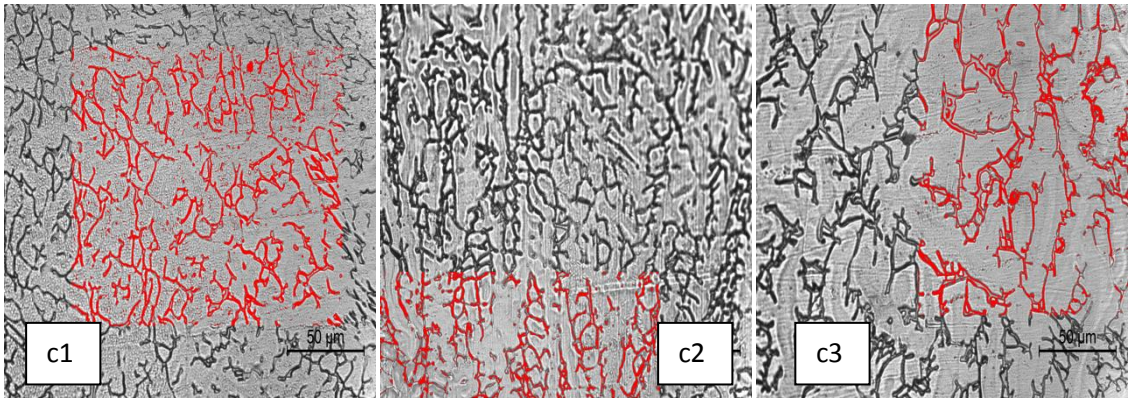

Fig.54 Delta ferrite dendrites of sample c1, c2 and c3

5.7 MICRO HARDNESS

Hardness values obtained at fusion zone, HAZ and at base metal are shown in fig. 55, 56 and 57.

From the obtained plots of hardness (Fig.55) it can be seen that samples welded at speed 1mm/s with less heat input has highest hardness at fusion zone and HAZ as compare to other heat input. And plots are also showing that as the heat input is increasing, the hardness of HAZ is more than fusion zone, at low heat input hardness at fusion zone is more than HAZ.

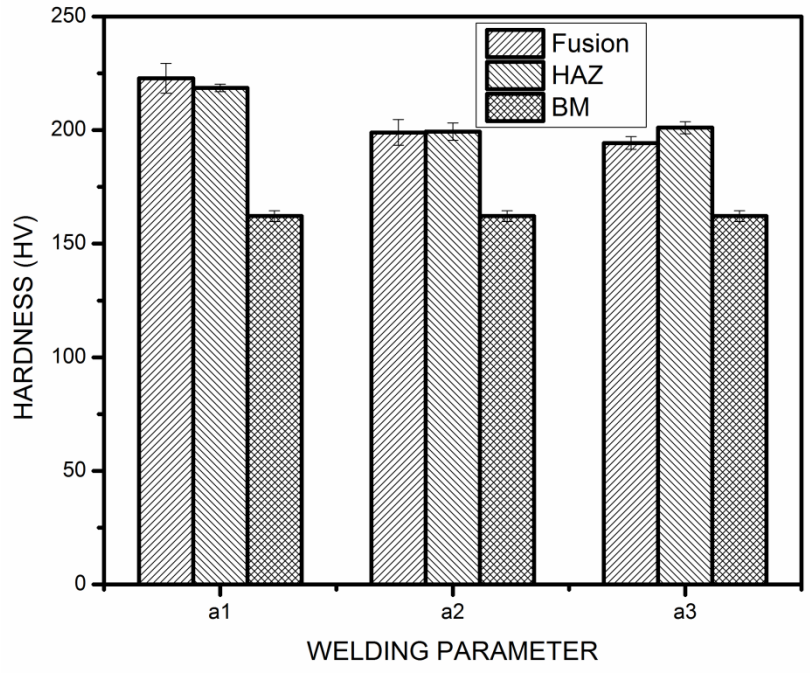

Fig.55 Micro hardness of sample a1, a2 and a3 at fusion zone, HAZ and base metal

Samples welded at 2mm/s and 3mm/s (Fig. 56 and fig. 58) also showing the same trend hardness values is increased at HAZ as comparison to fusion zone with the increase in heat input.

At HAZ it was found more hardness, it may be the reason that at high heat input there is sufficient time for cooling and sensitization may occur.

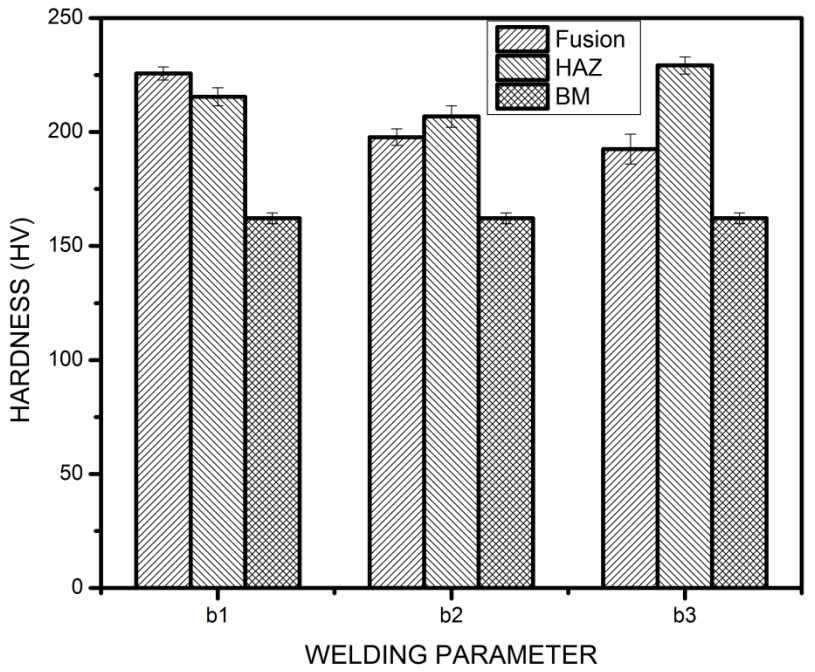

Fig.56 Micro hardness of sample b1, b2 and b3 at fusion zone, HAZ and base metal

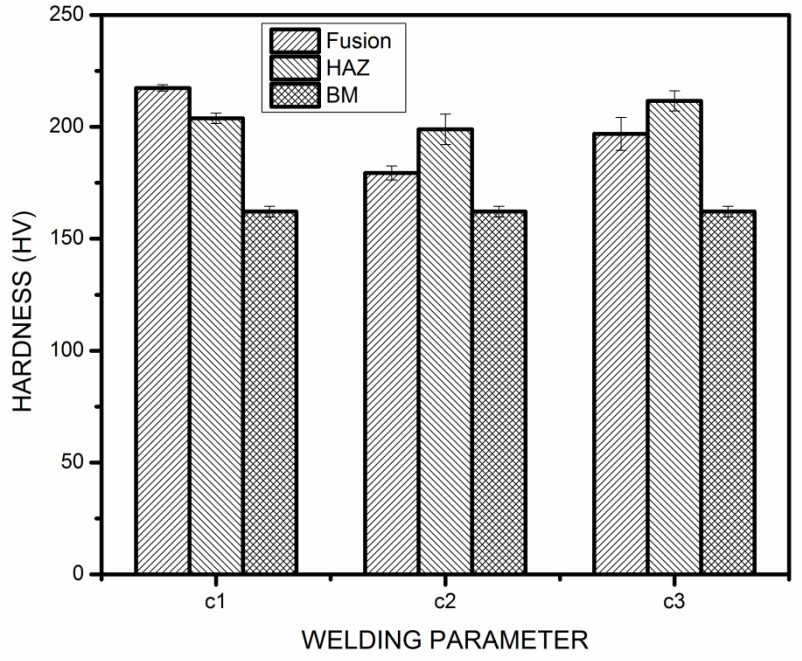

Fig.57 Micro hardness of sample c1, c2 and c3 at fusion zone, HAZ and base metal

Welding of SS 316 at a wide range of welding parameters was found beneficial as comparison to single set of welding parameter, since wide range of welding parameter including different welding speeds with different heat inputs gives more choice to select optimum welding parameter for the application.

Regarding investigation of microstructures it was found a variation of delta ferrite content with heat input at different welding speeds, which showed reduction in delta ferrite content with increment in heat input.

Investigation of corrosion behavior of all welded samples, reveled the corrosion characteristics. It was found that in OCP, linear polarization and in cyclic polarization test that optimum welding parameter was b3. Sample welded with b3 parameter showed good corrosion resistant results among other welding parameters.

Micro hardness test results showed a variation of hardness with welding speed increment as well as with heat input increment. At same welding speed hardness of fusion zone was decreased with increase in heat input, and at HAZ hardness was increased with higher heat input.

For future work, welding parameters could be controlled more precisely using same range of welding speeds for superior understanding against corrosion behavior.

EIS is a strong corrosion investigation technique; results obtained from EIS test could be analyzed more properly for correlation to literature.

Other mechanical property testing techniques could also be performed.

REFERENCES

[1] L.-M. Liu, S. T. Yuan, and C. B. Li, Effect of relative location of laser beam and TIG arc in different hybrid welding modes, *Sci. Technol. Weld. Join.*, 2012 vol. 17, no. 6, pp. 441–446.

[2] W.-S. Lee and C.-F. Lin, Impact properties and microstructure evolution of 304L stainless steel, *Mater. Sci. Eng. A*, 2001 vol. 308, no. 1–2, pp. 124–135.

[3] D. J. Lee, K. H. Jung, J. H. Sung, Y. H. Kim, K. H. Lee, J. U. Park, Y. T. Shin, and H. W. Lee, Pitting corrosion behavior on crack property in AISI 304L weld metals with varying Cr/Ni equivalent ratio, *Mater. Des.*, 2009 vol. 30, no. 8, pp. 3269–3273.

[4] H. U. Hong, B. S. Rho, and S. W. Nam, A study on the crack initiation and growth from δ-ferrite/γ phase interface under continuous fatigue and creep-fatigue conditions in type 304L stainless steels, *Int. J. Fatigue*, 2002 vol. 24, no. 10, pp. 1063–1070.

[5] C. Garcia, M. P. de Tiedra, Y. Blanco, O. Martin, and F. Martin, Intergranular corrosion of welded joints of austenitic stainless steels studied by using an electrochemical minicell, *Corros. Sci.*, 2008 vol. 50, no. 8, pp. 2390–2397.

[6] a Wahid, D. L. Olson, D. K. Matlock, C. E. Cross, M. Marietta, and A. Group, "Corrosion of Weldments," *ASM Handb.*, 1993 vol. 6, pp. 1065–1069.

[7] B. M. Ateša, I. S. Amardžić, and H.-S. Brod, Intergranular corrosion of dissimilar austenitic weld, 2012 vol. 54, no. 1, pp. 23–30.

[8] S. Edition, *Metallurgy Second Edition Welding Metallurgy*, vol. 822, no. 1–3. 2003.

[9] H. R. Z. Rajani, H. Torkamani, M. Sharbati, and S. Raygan, Corrosion resistance improvement in Gas Tungsten Arc Welded 316L stainless steel joints through controlled preheat treatment, *J. Mater.*, 2012 vol. 34, pp. 51–57.

[10] W. Chuaiphan and L. Srijaroenpramong, Effect of welding speed on microstructures, mechanical properties and corrosion behavior of GTA-welded AISI 201 stainless steel sheets, *J. Mater. Process. Technol.*, 2014 vol. 214, no. 2, pp. 402–408.

[11] M. G. Pujar, R. K. Dayal, S. N. Malhotra, and T. P. S. Gill, Evaluation of Microstructure and Electrochemical Corrosion Behavior of Austenitic 316 Stainless Steel Weld Metals with Varying Chemical Compositions, *J. Mater. Eng. Perform.*, 2005 vol. 14, no. 3, pp. 327–342.

[12] P. K. Giridharan and N. Murugan, Effect of Pulsed Gas Tungsten Arc Welding Process Parameters on Pitting Corrosion Resistance of Type 304L Stainless Steel Welds, *Corrosion*, 2007 vol. 63, no. 5, pp. 433–441.

[13] M. Dadfar, M. H. Fathi, F. Karimzadeh, M. R. Dadfar, and a. Saatchi, Effect of TIG welding on corrosion behavior of 316L stainless steel, *Mater. Lett.*, 2007 vol. 61, no. 11–12, pp. 2343–2346.

[14] S. K. Samanta, S. K. Mitra, and T. K. Pal, Microstructure and Oxidation Characteristics of Laser and GTAW Weldments in Austenitic Stainless Steels, *J. Mater. Eng. Perform.*, 2008 vol. 17, no. 6, pp. 908–914.

[15] S. Kumar and A. S. Shahi, Effect of heat input on the microstructure and mechanical properties of gas tungsten arc welded AISI 304 stainless steel joints, *Mater. Des.*, 2011 vol. 32, no. 6, pp. 3617–3623.

[16] X. M. Li, Y. Zou, Z. W. Zhang, Z. D. Zou, and B. S. Du, Intergranular corrosion of weld metal of super type 304H steel during 650??C aging, *Corrosion*, 2012 vol. 68, no. 5, pp. 379–387.

[17] A. Ravi Shankar, S. Niyanth, M. Vasudevan, and U. Kamachi Mudali, Microstructural characterization and corrosion behavior of activated flux gas tungsten arc-welded and multipass gas tungsten arc-welded stainless steel weld joints in nitric acid, *Corrosion*, 2012 vol. 68, no. August, pp. 762–773.

[18] A. A. O. Oyetunji A., Kutelu B. J., Effects of Welding Speeds and Power Inputs on the Hardness Property of Type 304L Austenitic Stainless Steel Heat - Affected Zone (HAZ), 2013 vol. 2, no. 4, pp. 124–129.

[19] Y. Lu, H. Jing, Y. Han, and L. Xu, Effect of Welding Heat Input on the Corrosion Resistance of Carbon Steel Weld Metal, *J. Mater. Eng. Perform.* 2015 vol. 11,no. pp. 237-242.

[20] A. A-canm, R. R. De Gouveia, A. Geraldo, M. Pukasiewicz, R. Capra, S. L. Henke, and P. C. Okimoto, "Effect of interpass temperature on microstructure , impact toughness and fatigue crack propagation in joints welded using the GTAW process on steel, 2105 vol. 7116, pp. 425-431.